Studies on the Magnetic Dichroism of Dye-Gelatin Films. III. Magnetic Dichroism of Dye-Gelatin Films Excited by Light

By Daijiro YAMAMOTO

(Received May 4, 1951)

In the previous papers[1][2] the magnetic dichroism of dye-gelatin films and its theoretical consideration have been reported. The magnetic dichroism in this case was due to diamagnetic orientation of dye-molecules, and its relaxation phenomena seemed to be due to the visco-elastic properties of solid gelatin.

If dye molecules were paramagnetic, the orientation would be changed, and the magnetic dichroism-time curves would alter their forms. During the last decade G. N. Lewis, M. Calvin, M. Kasha and their colabolators[3] have shown that organic molecules, having conjugated double bonds, turn into a phosphorescent state in rigid media by the illumination of visible and near ultraviolet rays, and its effect is due to a triplet state of π-electrons. Molecules in triplet state are paramagnetic, and these investigators confirmed the fact by determining the paramagnetic susceptibility of acid fluorescein dissolved in rigid boric acid glass by means of an excellent method using Theorell's micro balance.[4] This phenomenon is the so-called "Photomagnetism," named by them. Dye molecules have remarkable conjugated double bonds. Dye-gelatin films are also good phosphors[5]; in them, gelatin is to a certain extent a suitable rigid glassy solvent. Dye-gelatin phosphors may be due to a triplet state of π-electrons of double bonds.

From this view-point the author has examined the magnetic dichroism of dye-gelatin films excited by light, and obtained the following results.

Experimental

Materials.—The materials used were the same as mentioned in the previous paper. Dyes were dissolved in a gelatin-water solution at 50°, and smeared on glass plates and then dried. They were good phosphors. Nonphosphoric dyes like azo-dyes were also examined.

Apparatus.—All equipment is shown in Fig. 1. The magnet and measuring polarimeter were the same as mentioned in the previous paper, but the distance of the poles was taken as 7 mm. and all experiments were carried out under 9800 gauss (measured by fluxmetre). The sample was a strip of 6 mm. × 20 mm. and it was set in a magnetic field, whose direction was parallel to the surface of the film. The exciting light source was a 6~8 amp. carbon arc or a mercury lamp. Between the light source and the sample along the optical path were set filters of water, $CuSO_4$-water solution, $CuCl_2$-alcohol solution or colored glass filters for each purposes. The excitation of materials by light was carried out by a uniform image of diaphragm projected on the film. The opening of the diaphragm was 10 mm.×10 mm., and the size of the image was 6 mm.×6 mm.

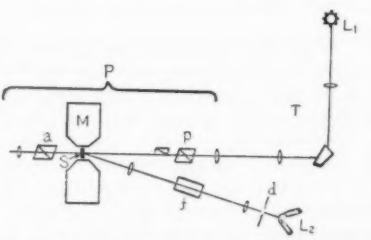

Fig. 1.—Schematic diagram of the equipment for studying the magnetic dichroism: S, sample; P, polarimeter; M, magnet; T, monochrometer; L_1, measuring light source; L_2, exciting light source; p, polariser; a, analyser; f, filter; d, diaphragm.

Dichroism was measured by means of the polarimeter which F. Weigert[6] used for his studies on the photodichroism. In this method dichroism D is given according to the following relation,

$$D = 2 \log \tan (45° \pm \alpha) = 0.015 \times 2\alpha$$

where α is the angle of rotation of the analyser.

Difficulties in the Experiments.—There are many difficulties in this experiment. They are as follows:

(1) D. Yamamoto, *J. Chem. Soc. Japan.* **72**, 693 (1951).
(2) D. Yamamoto, *ibid.*, **72**, 782 (1951)
(3) Their works have been summarized by M. Kasha, *Chem. Rev.*, **41**, 401 (1947).
(4) G. N. Lewis, M. Calvin and M. kasha, *J. Chem. Phys.*, **17**, 804 (1949).
(5) *e. g.*, P. Fröhlich and Z. Gyulai, *Z. Phys.*, **104**, 549 (1937). Now in the author's laboratory dye-gelatin phosphors are being studied by the author with Mr. R. Iwaki.
(6) F. Weigert, *Z. Physik. Chem.*, (B) **3**, 377, (1929).

(1) Dyes are decomposed by light (bleaching or discoloring), especially by near ultraviolet rays.

(2) Phosphorescence and fluorescence of films lead to errors in measured values of dichroism.

(3) Absorption bands of dyes are not necessarily in a suitable position for excitation.

The Difficulty of (1) is removed by using proper filters, and the author's studies on the photodichroism of such materials make clear the effect of bleaching or discoloring in dyes, so we are able to know the most suitable condition for experiments.[7] (2) is very troublesome because of the interruption of the measuring light, so that monochromatic rays for observation diminish. But if we use such materials as phosphorecent bands in long wave length region *e. g.* orange or red, and if their intensities are weak, we can read the correct value of dichroism. (3) is not so troublesome, for we can choose proper materials which have absorption band in the vicinity of 430 or 546 mμ for mercury lamp. But in practice the intensity of a mercury lamp is not very satisfactory, so that an arc light and proper filters are used for examination after testing by the monochromatic rays of a mercury lamp.

Results Obtained

Results obtained on the malachite green, rhodamine-B, fuchsine, fluorescein, pinachrome, pinacyanol, azo-dyes *e. g.* chrysoidine, congo red-gelatin films were as follows:

(1) **1.25% Malachite Green-Gelatin Film.**—Malachite green-gelatin film has an absorption band near 620 mμ[8] which is due to shift of π-electron. By intense illumination of red rays (600~650 mμ, filter: red glass+water) dark deep red phosphorescence[9] (probably about 700~800 mμ) is found. There was no discoloring by excitation for 10 minutes, and it is confirmed by means of a study on photodichroism. Magnetic dichroism—time curves are shown in Fig. 2. A curve in no excitation was the same as mentioned in the previous papers. But by excitation of red rays, curves had altered their shapes as seen in the figure. As soon as the exciting light was shut off the value of dichroism came back rapidly to that of mere magnetic dichroism.

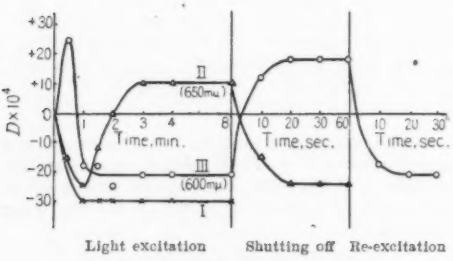

Fig. 2.

In Fig. 2, curve I is due to mere magnetic dichroism, and its dichroism is measured by 650 mμ, curve II is due to the excitation by red rays and measured by 650 mμ, and curve III is due to the same exciting light, but measured by 600 mμ. The opposite sign is due to dispersion. The dispersion of magnetic dichroism in both non-exciting and exciting states was examined. Results obtained are shown in Fig. 3. Both curves are in relation to mirror images.

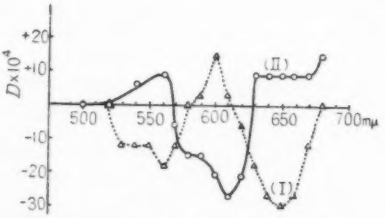

Fig. 3.—Dispersion of dichroism: (I), non-excitation; (II), excitation.

(2) **1.25% Rhodamine B-Gelatin Film.**—Rhodamine B-gelatin film has a green absorption band, and its phosphorescence is orange-red. As exciting light, the following filters were used. (1) $CuSO_4$-water for 546 mμ Hg, (2) blue glass+water, (3) $CuCl_2$-alcoholic solution and (4) blue glass+$K_2Cr_2O_7$-water for arc light. In each case phosphorescence was visual, and so measuring was hard. (Bleaching was not found.) The effect is evident in the case of filter (2), (3) and (4). Results obtained are shown in Fig. 4. Dispersion of both states is shown in Fig. 5.

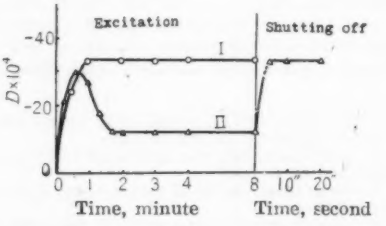

Fig. 4.—(I), non-excitation; (II), excited by blue light (filter No. 2), measured by 560 mμ.

(7) D. Yamamoto and R. Iwaki, *J. Chem. Soc., Japan*, **72**, 852, 854 (1951).

(8) Absorption bands of following dye-gelatin films were given by unpublished works of Mr. R. Iwaki.

(9) Phosphorescence of dye-gelatin films was examined by 1800 r. p. m. phosphorscope.

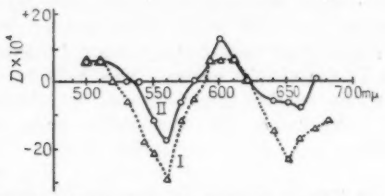

Fig. 5.—Dispersion of dichroism; (I), non-excitation; (II), excited by green light (filter No. 4).

(3) **1% Fuchsine-Gelatin Film.**—Fuchsine-gelatin film has an absorption band near 546 mμ Hg. Phosphorescence is yellowish orange. The effect of excitation by green light was evident. One of the results is shown in Fig. 6.

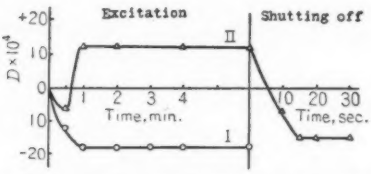

Fig. 6.—(I), non-excitation; (II), excited by green light.

(4) **0.75% Fluorescein-Gelatin Film.**—Fluorescein- and uranin (Na-fluorescein)-gelatin films are not so good as phosphors. They show, however, the effect by the excitation of blue light. They have absorption bands in 480~490 mμ. Excitation by 490 mμ Hg is suitable, but it is so weak that it can not be used for excitation. Then, excitation by blue light (blue glass+water, arc light) showed the effect. Results obtained are shown in Fig. 7.

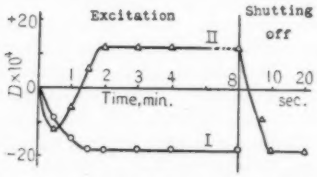

Fig. 7.—(I), non-excitation; (II), excited by blue light, measured by 570 mμ.

(5) **Cyanine Dyes-Gelatin Films.**—1.25% Pinachrome- and 1.25% pinacyanol-gelatin films were examined. They showed weak phosphorescence. Pinachrome-gelatin films showed effect by excitation of blue light, and pinacyanol-gelatin films by red light. But in them slight bleaching was observed.* Results are shown in Figs. 8 and 9.

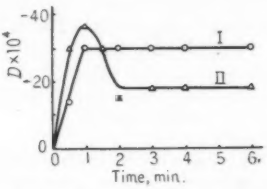

Fig. 8.—1.25% Pinachrome-gelatin film: (I), non-excitation; (II), excited by blue light, measured by 610 mμ.

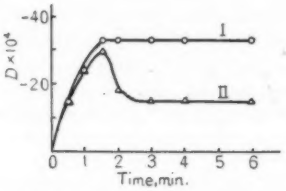

Fig. 9.—1.25% Pinacyanol-gelatin film: (I), non-excitation; (II), excited by red rays, measured by 580 mμ.

(6) **Azo-dyes-Gelatin Films.**—For azo-dyes chrysoidine and congo red were used. Azo-dyes-gelatin films are non-phosphors and they show strong bleaching by illumination of light. Chrysoidine is a very simple monoazo-dye, on the other hand, congo red is a very complicated disazo-dye. On 1% chrysoidine-gelatin film

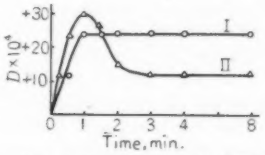

Fig. 10.—1% Chrysoidine-gelatin film: (I), non-excitation; (II), excited by blue light (without water filter), measured by 550 mμ.

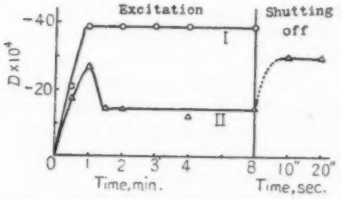

Fig. 11.—1.5% Congo red-gelatin film: (I), non-excitation; (II), excited by blue light, measured by 580 mμ.

the effect was not distinct. 1.5% congo red-gelatin film showed the effect by excitation of blue light, but after shutting off the light the value of dichroism did not come back to that of mere magnetic dichroism. These results are shown in Figs. 10 and 11.

Summary

There were found considerable changes in magnetic dichroism of some dyes-gelatin films by excitation of light. In malachite green and rhodamine B-gelatin films this effect was very evident, and cyanine dyes-and azo-dyes-gelatin films also showed the same effect. This effect may have something to do with the phosphorescent state of dye molecules, having conjugated double bonds, but nothing to do with bleaching by light. Azo-dyes-gelatin films are non-phosphors, but G. N. Lewis and M. Kasha[10] thought that these materials would have a phosphorescent band in near infra red regions. It is difficult to decide between phosphor and non-phosphor by limited observation in the visible region. This will be discussed in another paper if those experimental results are due to photomagnetism or to other causes.

The author wishes to express his sincere thanks to Prof. Jitaro Shidei for his kind guidance and to Mr. Ryojiro Iwaki for his valuable discussions of these problems, and also to the Ministry of Education for grants in aid out of the Scientific Research Expenditure.

Department of Chemistry, Faculty of Science,
Tokyo University of Education,
Otsuka, Tokyo

(10) G. N. Lewis and M. Kasha, *J. Amer. Chem. Soc.*, **66**, 2100 (1944).

Studies on the Magnetic Dichroism of Dye-Gelatin Films. IV. Confirmation of Photomagnetism by means of Magnetic Dichroism in Dye-Gelatin Films Excited by Light

By Daijiro YAMAMOTO

(Received May 4, 1951)

In the last paper[1] the author reported the changes of magnetic dichroism of dye-gelatin films by excitation of light. As to the cause of this effect, the author briefly pointed out elsewhere that this effect would be due to photomagnetism of dye molecules in solid gelatin.[2] But its treatment did not include the saturation effect of excited molecules, and the ground conception of the mechanism of magnetic dichroism was not so correct. The author[3] made phenomenologically a theoretical consideration on the magnetic dichroism of dye-gelatin films as visco-elastic properties of gelatin, taking phosphorescence and photo-dichroism into consideration. In the visco-elastic model entropy-elasticity of chains in net-work structure of gelatin was assumed. This conception would not be so correct. But the results obtained by such a conception could explain the relaxation phenomena well, and the dichroism--time relations accorded with experimental results very well. In an ordinary way, magnetic dichroism is due to diamagnetic orientation, but in the case of paramagnetic molecules, the orientation may differ from diamagnetic ones, and dichroism-time relations are also different. The author obtained a distribution function for paramagnetic orientation and combined it with a diamagnetic one, and then obtained dichroism-time relations in co-existent state of dia- and paramagnetism. These relations can well explain qualitatively the experimental results, reported in the preceding paper. So the author supposes that the differences which appeared in magnetic dichroism-time relations by the excitation of light would be due to the photomagnetism effect, discovered by G. N. Lewis, M. Calvin and M. Kasha[4].

(1) D. Yamamoto, This Bulletin, **24**, 211 (1951).
(2) D. Yamamoto, *Kagaku (in Japanese)*, **20**, 574 (1950).
(3) D. Yamamoto, *J. Chem. Soc. Japan*, **72**, 782 (1951).
(4) G. N. Lewis, M. Calvin and M. Kasha, *J. Chem. Phys.*, **17**, 804 (1949).

Theoretical

Distribution Function in Paramagnetic Orientation.—As in the previous case, the author took the following four assumptions in dye-gelatin systems:

(1) Gelatin has a net-work structure and elements of a chain are allowed of micro-brownian motion to some extent. In this, entropy-elasticity is assumed.

(2) One of dye molecules attaches to one element, and its combination is fairly strong, but weaker than valence combination.

(3) Paramagnetic action of dye molecules in magnetic field is stronger than diamagnetic action of chain, so we neglect the diamagnetic orientation of chains.

(4) By the orientation of dyes, combined elements are set in rotation, and then the elongation or compression in neighboring chains of those elements appears. But in that case knots of network do not slide.

According to those assumptions, the following phenomenological equations were taken for the rotation of dye molecules;

$$\left.\begin{aligned} \frac{d\vartheta}{dt} &= \frac{2}{a\cdot G}\cdot\frac{dF_1}{dt} \\ \frac{d\vartheta}{dt} &= \frac{2}{a\cdot\eta}\cdot F_2 \\ F_1+F_2 &= M/a \times\gamma \end{aligned}\right\} \quad (1)$$

where a is the diameter of a sphere, regarding a molecule with a combined element as a sphere, ϑ is the angle of rotation of a sphere, G is the mean elastic constant, η is the viscosity for inner flow, M is the moment of rotation, γ is a correction term which has the value of $0<\gamma<1$, presumably it is proper to take about $1/3$, and F_1 and F_2 are components for elastic and viscous action. This relation is Voigt's parallel model for visco-elastic system.

Distribution function f is represented by the following differential equation with time, as mentioned in the previous treatment.

$$\frac{\partial f}{\partial t} = -\left\{\frac{2\gamma\cdot M}{a^2\eta}\cdot\exp(-G/\eta\cdot t)\right\} \times\frac{1}{\sin\theta}\cdot\frac{\partial}{\partial\theta}(\sin\theta\cdot M\cdot f) \quad (2)$$

where θ is the angle between direction of paramagnetic dipole moment and magnetic field. We can obtain a distribution function by solving this equation under given moment of rotation M. Moment M is given by the following relation for paramagnetic dipole

$$M = d\cdot H\cdot\sin\theta$$

where d is a constant proportional to the magnitude of paramagnetic dipolemoment of dye molecule and H is the strength of magnetic field in gauss.

Distribution function is usually represented by the following expanded series:

$$f=\frac{1}{4\pi}\{1+A_1P_1(\cos\theta)+A_2P_2(\cos\theta)+\cdots\cdot\} \quad (3)$$

where P_1, P_2, ... are Legendre's spherical functions and A_1, A_2, ... are constants without θ. By the second order approximation, we can write a distribution function f_{para} for paramagnetic orientation as follows

$$f_{para}=\frac{1}{4\pi}\{1+R(t)P_1(\cos\theta)+S(t)P_2(\cos\theta)\} \quad (4)$$

where $R(t)$ and $S(t)$ are functions with time. They are obtained approximately by the following method. At first $R(t)$ is obtained by the first order approximation;

$$f_{para}=\frac{1}{4\pi}\{1+R(t)P_1(\cos\theta)\} \quad (5)$$

Combining Eqs. (2), (5) and relation $P_1(\cos\theta)=\cos\theta$, we obtained $R(t)$ as follows.

$$R(t)=-\frac{2\gamma\cdot d\cdot H}{a^2G}\{1-\exp(-G/\eta\cdot t)\} \quad (6)$$

Next, we take the second order approximation as

$$f_{para}=\frac{1}{4\pi}\{1+R(t)P_1(\cos\theta)+S(t)P_2(\cos\theta)\} \quad (7)$$

and by (2), (6), (7) and use $P_2(\cos\theta)=1/2\times(3\cos^2\theta-1)$, we obtain the following equation;

$$\frac{dS(t)}{dt}=-\frac{2\gamma\cdot d\cdot H}{a^2\eta}\cdot\exp(-G/\eta\cdot t)\cdot R(t). \quad (8)$$

By introducing (6) in (8), we obtain the following equation for $S(t)$

$$S(t)=\frac{4\gamma^2d^2H^2}{a^4G\cdot\eta}\{1-\exp(-G/\eta\cdot t)\}^2. \quad (9)$$

So we obtain the distribution function for paramagnetic orientation as follows:

$$f_{para}=\frac{1}{4\pi}\left\{1-\frac{2\gamma dH}{a^2G}[1-\exp(-G/\eta\cdot t)]\times P_1(\cos\theta)+\frac{4\gamma^2d^2H^2}{a^4G\eta}[1-\exp(-G/\eta\cdot t)]^2P_2(\cos\theta)\right\}. \quad (10)$$

On the other hand, the distribution function for diamagnetic orientation f_{dia} is as follows, as mentioned in a previous paper;

$$f_{dia}=\frac{1}{4\pi}\left\{1+\frac{2\gamma bH^2}{a^2G}[1-\exp(-G/\eta\cdot t)]\cdot P_2(\cos\theta)\right\}, \quad (11)$$

where b is a diamagnetic constant depending on the diamagnetic susceptibility of a dye molecule.

Magnetic Dichroism—Time Relations for Paramagnetic Molecules.—Prior to the consideration for magnetic dichroism in co-exsistent state of dia- and paramagnetic molecules, magnetic dichroism owing merely to paramagnetic molecules are treated. If paramagnetic molecules have molecular dichroism ($\alpha_1'-\alpha_2'$) in voluntary measuring wave length, in which α_1' is the molecular extinction coefficient parallel to the dipole moment and α_2' is one perpendicular to the α_1' direction. This conception is the same as used by W. Kuhn *et al.*,[5] for exposition of electric dichroism of dye molecules.

Let α_p' be parallel component along to the direction of magnetic field H_z, directions perpedicular to H_z are H_y and H_x, and component α_s' be along the direction H_y, direction of observation is parallel to H_x, and φ be the angle between α_2' and H_y as shown in Fig. 1, the following equations are obtained.

$$\alpha_p'=(\alpha_1'-\alpha_2')\cos^2\theta+\alpha_2'$$
$$\alpha_s'=(\alpha_1'-\alpha_2')\sin^2\theta\cos^2\varphi+\alpha_2'.$$

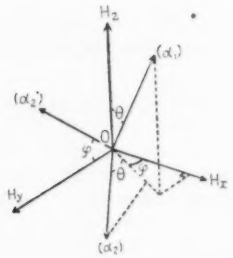

Fig. 1.

(5) W. Kuhn, H. Dürkop and H. Martin, *Z. physik. Chem.*, (B) **45**, 121 (1939).

So, the factor of dichroism for a molecule $\alpha_p'-\alpha_s'$ is as follows:

$$\alpha_p'-\alpha_s'=(\alpha_1'-\alpha_2')(\cos^2\theta-\sin^2\theta\cdot\cos^2\varphi). \quad (12)$$

Dichroism of a film is represented by the following relations for N-molecules (in the material used $N=c\cdot l$, where c is mol concentration per cm^2., and l is thickness of film in cm.)

$$D=N\int(\alpha_p'-\alpha_s')f\,d\Omega$$
$$=\frac{N}{4\pi}\int_{\varphi=0}^{2\pi}\int_{\theta=0}^{\pi}(\alpha_1'-\alpha_2')(\cos^2\theta-\sin^2\theta\cdot\cos^2\varphi)\times\{1+R(t)P_1(\cos\theta)+S(t)P_2(\cos\theta)\}\sin\theta\cdot d\theta\cdot d\varphi, \quad (13)$$

where Ω is solid angle involving θ. While

$$\iint(\cos^2\theta-\sin^2\theta\cdot\cos^2\varphi)\sin\theta\cdot d\theta\cdot d\varphi=0$$
$$\iint P_1(\cos\theta)(\cos^2\theta-\sin^2\theta\cdot\cos^2\varphi)\sin\theta\cdot d\theta\cdot d\varphi=0$$
$$\iint P_2(\cos\theta)(\cos^2\theta-\sin^2\theta\cdot\cos^2\varphi)\sin\theta\cdot d\theta\cdot d\varphi=\frac{4}{5}\pi.$$

so we obtain for dichroism D the following formulas

$$D=\frac{1}{5}N(\alpha_1'-\alpha_2')S(t)$$
$$=\frac{4}{5}N(\alpha_1'-\alpha_2')\cdot\frac{\gamma^2d^2H^2}{a^4G\eta}\times\{1-\exp(-G/\eta\cdot t)\}^2 \quad (14)$$
$$=D_{\infty\cdot para}\{1-\exp(-t/\tau)\}^2, \quad (15)$$

where $D_{\infty\cdot para}$ is the value of dichroism for $t=\infty$.

Magnetic Dichroism—Time Relations in the Case of Co-existence of Dia- and Paramagnetic Molecules.—In the case of diamagnetic orientation D is given by the following equation after distribution function f_{dia}, as mentioned in the previous paper,

$$D_{dia}=D_\infty\{1-\exp(-t/\tau)\} \quad (16)$$

where $1/\tau=G/\eta$.

On the other hand, in the case of co-existence of both states, two factors should be considered. One of them is the degree of

saturation, *i. e.*, paramagnetic molecules/total molecules, and the other is molecular dichroism of paramagnetic state. If the saturation factor is put ξ, the number of paramagnetic molecules is $N\xi$, and the number of diamagnetic molecules is $N(1-\xi)$, and they are in equilibrium. As the life time of excited state τ' is shorter than relaxation time of magnetic dichroism, *i. e.*, $\tau' \ll \tau$, orientation is governed by $(1-\xi)N's$ diamagnetic molecules and $N\xi$ paramagnetic molecules statistically, so dichroism observed is as follows;

$$D_{dia}=(1-\xi)^2 D_{\infty\cdot dia}\{1-\exp(-t/\tau)\} + (1-\xi)\xi\cdot D'_{\infty\cdot dia}\{1-\exp(-t/\tau)\} \quad (17)$$

for molecules in diamagnetic part, and

$$D_{para}=(1-\xi)\cdot\xi\cdot D_{\infty\cdot para}\{1-\exp(-t/\tau)\}^2 + \xi^2 D'_{\infty\cdot para}\{1-\exp(-t/\tau)\}^2 \quad (18)$$

for paramagnetic part, after Eqs. (15) and (16), where

$$D_{\infty\cdot dia}=\frac{4}{5}N(\alpha_1-\alpha_2)\cdot\frac{\gamma b H^2}{a_2 G}, \quad (19)$$

$$D_{\infty\cdot para}=\frac{4}{5}N(\alpha_1-\alpha_2)\cdot\frac{\gamma^2 d^2 H^2}{a^4 G\cdot\eta}, \quad (20)$$

$$D'_{\infty\cdot dia}=\frac{4}{5}N(\alpha_1'-\alpha_2')\frac{\gamma b H^2}{a^2 G} \quad (21)$$

$$D'_{\infty\cdot para}=\frac{4}{5}N(\alpha_1'-\alpha_2')\frac{\gamma^2 d^2 H^2}{a^4 G}, \quad (22)$$

and $(\alpha_1-\alpha_2)$ is molecular dichroism for a diamagnetic molecule, and $(\alpha_1'-\alpha_2')$ is for paramagnetic molecules. In dye-gelatin phosphors, ξ is not so large that we are able to neglect ξ^2 for ξ. So we can neglect the second term of Eq. (18). By combining the two cases, we obtain the following relation in the case of co-existence of both states.

$$D=(1-\xi)[(1-\xi)D_{\infty\cdot dia}\{1-\exp(-t/\tau)\} + \xi\cdot D_{\infty\cdot para}\{1-\exp(-t/\tau)\}^2 + \xi\cdot D'_{\infty\cdot dia}\{1-\exp(-t/\tau)\}]. \quad (23)$$

Comparison with Experimental Results

On Eq. (23), we consider two processes to compare theoretical works with experimental results.

(1) **In the Case of** $(\alpha_1'-\alpha_2')=0$.--At first we consider the case of $D'_{\infty\cdot dia}=0$, *i. e.*, $(\alpha_1'-\alpha_2')=0$. In this case, Eq. (23) is taken as follows :

$$D=(1-\xi)\cdot D_{\infty\cdot dia}[(1-\xi)\{1-\exp(-t/\tau)\} + \xi\cdot D_{\infty\cdot para}/D_{\infty\cdot dia}\times\{1-\exp(-t/\tau)\}^2] \quad (24)$$

In the dye-gelatin phosphors, ξ is very small in comparison with dye-boric acid glass phosphor, so we are able to put it down as follows, for $(1-\xi)\fallingdotseq 1$:

$$D=D_{\infty\cdot dia}[\{1-\exp(-t/\tau)\} + \xi\cdot D_{\infty\cdot para}/D_{\infty\cdot dia}\times\{1-\exp(-t/\tau)\}^2]. \quad (25)$$

For various values of $\xi\cdot D_{\infty\cdot para}/D_{\infty\cdot dia}$, curves of (25) are shown in Fig. 2. As $b<0$, and $(d^2)>0$, so the sign of $D_{\infty\cdot para}/D_{\infty dia}$ is negative.

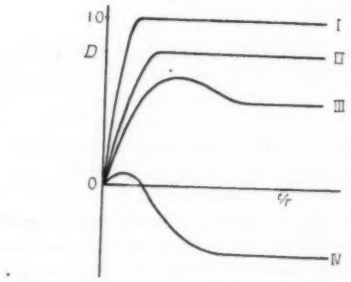

Fig. 2.—$\xi D_{\infty\cdot para}/D_{\infty\cdot dia}=$: I, 0; II, $-1/5$; III, $-1/2$; IV, $-7/5$.

(2) **In the case of** $(\alpha_1'-\alpha_2')\neq 0$. — If $\xi D'_{\infty\cdot dia}$ is fairly large, the term $\xi D'_{\infty\cdot dia}/D_{\infty\cdot dia}\cdot\{1-\exp(-t/\tau)\}$ is added into Eq. (25):

$$D=D_{\infty\cdot dia}[\{1-\exp(-t/\tau)\} + \xi\cdot D'_{\infty\cdot dia}/D_{\infty\cdot dia}\cdot\{1-\exp(-t/\tau)\} + \xi\cdot D'_{\infty\cdot para}/D_{\infty\cdot dia}\{1-\exp(-t/\tau)\}^2] \quad (26)$$

and its curves are changed into what is shown in Fig. 3, for some cases.

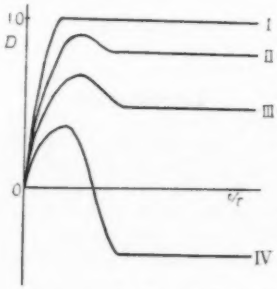

Fig. 3.—The case of $D'_{\infty\cdot dia}/D_{\infty}=1/10\sim 1/2$; I, II, III and IV correspond to I, II, III and IV in Fig. 2 respectively.

Experimental results as mentioned in the preceding paper on the malachite green-, fuchsine and fluorecein-gelatin films are in good accordance with curve IV in Fig. 3, and results on the other dyes-gelatin films with curve III in Fig. 2 or curve III in Fig. 3, in the range of measuring errors. In the former there may be molecular dichroism in paramagnetic molecules, in the measuring wave length.

Behavior in the Case of Shutting off the Excitation of Light

By shutting off the excitation of light, the value of dichroism returns rapidiy to that of mere magnetic dichroism. Its behavior is represented by the following equation, after Eq (25) or (26).

$$D=D_{\infty\cdot dia}[1+\xi\cdot D_{\infty\cdot para}/D_{\infty\cdot dia}\cdot\exp(-t/\tau')] \tag{27}$$

or

$$D=D_{\infty\cdot dia}[1+\xi\cdot D_{\infty\cdot para}/D_{\infty\cdot dia}\cdot\exp(-t/\tau') + \xi\cdot D'_{\infty\cdot dia}/D_{\infty\cdot dia}\cdot\exp(-t/\tau')] \tag{28}$$

where τ' is the mean life time of paramagnetic molecules. So, in this effect, relaxation time is equal to the life time of paramagnetic molecules. Experimental results mentioned before are in good accordance with this consideration, in the range of measuring errors.

Quantitative Considerations

It is very difficult to compare theoretical calculations with experimental results, and to get an accurate value of d, the important value for paramagnetic dipole moment. Because in the case of mere magnetic dichroism, G and η were not such suitable values for the materials used.

Summary

The Differences which appeared in the magnetic dichroism-time relations of dye-gelatin films by excitation of light were discussed under assumption of photomagnetism effect. Results obtained are to some extent in good accordance with experimental results qualitatively. The author, however, can not decide that this effect is entirely due to the photomagnetism. It will be valid, to some extent, to regard the effect to be due to photomagnetism.

The author wishes to thank Prof. Jitaro Shidei for his good guidances throughout this work, Mr. Ryojiro Iwaki for his valuable discussions and encouragement on this topic and also the Ministry of Education for grant in aid out of the Scientific Research Expenditure.

Department of Chemistry, Faculty of Science,
Tokyo University of Education,
Otsuka, Tokyo

Research on Activation Energy. I. A New Empirical Rule for the Calculation of Activation Energy[1]

By Kiyoteru Otozai

(Received May 8, 1951)

Introduction

Because of the difficulty of calculating in a solely theoretical way the activation energy for any sort of reaction, various kinds of empirical or semi-empirical rules have been proposed for the estimation of that energy. The general feature of the purely empirical rules so far proposed is the simplicity of their forms. But at the same time they can be applied only to a specified type of reaction. Moreover, none of these empirical rules provide any information on the geometrical configuration of the activated complex. Compared with these purely empirical methods, the so-called semi-empirical method of Eyring has a marked advance. It can be applied not only to any kind of reaction but it also enables us to presume the geometrical configuration and the

(1) Details will be publisled in Scientific Papers from the Osaka University.

dimensions of the activated complex. But unfortunately the estimation of the constant ρ, which represents a fraction of the Coulombic part in the total energy of the bond, and the knowledge of which is always necessary for the calculation of the activation energy according to this method, is at least at present not quite free from ambiguity. For this reason the author has sought a new empirical method of calculation, which makes use only of the experimentally measurable constants but gives us almost as accurate information as the semi-empirical method on the magnitude of the activation energy and the geometrical dimensions of the activated complex. The method reported here is one such which satisfies the above-mentioned requirements, although the theoretical basis for the calculation is not yet quite clear.

Fundamental Assumption

The distance r^*, which corresponds to the inflexion point on the potential-energy curve or the point, where the attractive force between two atoms becomes maximum, (cf. Fig. 1), is

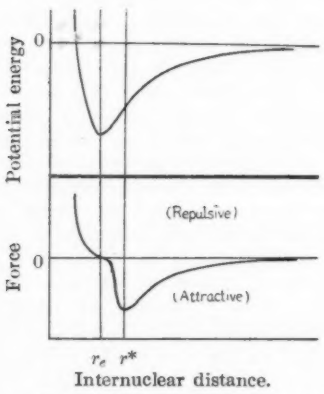

Fig. 1.—The activated internuclear distance.

assumed to represent the length of the bond in an activated complex. This distance r^* will, therefore, be called the activated internuclear distance. Furthermore we will denote the bond, which appears only in an activated complex (see below) an activated bond. Then the present empirical rule can be summarized as follows: among all the possible structures, which can be constructed by the use of the fixed values of the activated internuclear distances of the bonds to be broken as well as to be formed, such a structure, in which the sum of the energies of the activated bonds becomes minimum, represents the structure of the activated complex and this minimum sum of the energies of the activated bonds gives the activation energy of the reaction, when it proceeds in the exothermic direction. The activation energy of the reaction in the endothermic direction can readily be calculated by the use of the so computed value of the activation energy in the exothermic direction and the heat of the reaction.

Thus, for the tetratomic reaction of the type:

the bonds to be broken are X–Y and W–Z, those to be formed are X–W and Y–Z and the activated bonds, which appear only in an activated complex, are X...Z and Y...W. Hence, according to the present rule, among all the possible structures, which can be constructed by the use of the fixed values of the activated internuclear distances r^*_{XY}, r^*_{YZ}, r^*_{ZW}, and r^*_{WX}, such a structure, in which the sum of the energies of the activated bonds X...Z and Y...W becomes minimum, represents the structure of the activated complex, and this minimum sum of the energies gives the activation energy of the reaction, when it proceeds in the exothermic direction.

Carrying out the Calculation

One of the most important parts of the calculation according to the present rule is the determination of the potential-energy $U(r)$ between two atoms as a function of their internuclear distance. But as the ordinarily used Morse's equation was found not accurate enough for this purpose (see below), we have made use of Rydberg's equation:[2]

$$U(r) = -D_e\{a(r-r_e)+1\}e^{-a(r-r_e)},$$

in which D_e is the equilibrium dissociation energy, a is the characteristic constant for the given pair of atoms and r_e is the equilibrium internuclear distance. All of these constants can be calculated from the spectroscopic data according to the equations:

$$D_e = D + E_0,$$

(2) R. Rydberg, *Z. Phys.*, **73**, 381 (1932).

$$E_0=\frac{1}{2}N\,k\nu=1.45\times10^{-3}\omega_e,$$

$$a=9.28\times10^{-3}\omega_e\sqrt{\mu/D_e},$$

where E_0 represents the zero point energy and μ the reduced mass of the pair of atoms. Furthermore, it can readily be shown from Rydberg's equation that the activated distance r^*, which corresponds to the inflexion point on the potential energy curve, is expressed by the equation:

$$r^*=r_e+1/a.$$

The activation energies of some triatomic and tetratomic reactions calculated according to the present method are summarized in Tables 1 and 2 respectively, and compared with the experimental values given in the textbook of Glasstone, Laidler and Eyring[3] as well as the values calculated by means of the semiempirical method of Eyring, where the energies are all expressed in kcal. units.

Table 1

Activation Energies of Some Triatomic Reactions

No.	Reaction	Activation energy: Observed	Calculated: i	Calculated: ii
1	$H+p-H_2\rightarrow o-H_2+H+0$	7	10.1	7.63 (20%)
2	$H+I_2\rightarrow HI+I+35$	0	0.2	2.5 (10%) 1.8 (14%)
3	$I+H_2\rightarrow IH+H-32$	34.2	41.2	43.3 (10%) 40.4 (14%)
4	$H+Br_2\rightarrow HBr+Br+41$	1.2	0.3	3 (10%) 2.1 (14%)
5	$Br+H_2\rightarrow BrH+H-16$	18	23.2	25.5 (20%)
6	$H+Cl_2\rightarrow HCl+Cl+45$	2	0.7	2.7 (14%)
7	$Cl+H_2\rightarrow ClH+H-1$	6	9.0	11.6 (20%)
8	$F+H_2\rightarrow FH+H+45$	8	10.4	10.6 (10%) 6.3 (14%)

i, according to the present method.
ii, according to the semi-empirical method of Eyring, where the number in bracket indicates the value of the constant ρ used for the respective calculation.

(3) G. Glasstone, K. J. Laidler and H. Eyring, "The Theory of Rate Processes", McGraw-Hill Company, New York and London, 1941.

Table 2

Activation Energies of Some Tetratomic Reactions

No.	Reaction	Activation energy: Observed	Calculated: i	Calculated: ii
1	$H_2+H_2\rightarrow H_2+H_2+0$	>59	76.4	*ca.* 90 (10%)
2	$H_2+I_2\rightarrow 2HI+3$	40	38.2	48.3 (14%)
3	$H_2+Br_2\rightarrow 2HBr+25$	>43	41.8	45 (10%) 39 (14%) 26.5 (20%)
4	$H_2+Cl_2\rightarrow 2HCl+44$	>36	51.0	54 (10%) 44.5 (14%) 29.5 (20%)
5	$H_2+F_2\rightarrow 2HF+129$	>25	92.2	50 (10%)
6	$Br_2+Cl_2\rightarrow 2BrCl+1$	14	11.3	—
7	$D_2+HCl\rightarrow HD+DCl+0$	57	*ca.* 58	53 (17%) 43.6 (20%)

Discussion of Errors

When the results shown in Table 1 are compared with those in Table 2, it may be seen that the activation energies calculated according to the present method are generally somewhat too high (in the average about 3 kcal.) in comparison with the experimental values for the triatomic reactions (except for the endothermic reactions), while just the reverse is the case for the tetratomic reactions. However, the same tendency can also be seen for the values calculated by means of the semi-empirical method, although in this case the adequate choice of the constent ρ makes this difference somewhat obscure. Just this tendency seems to betray the difficulty in calculating the activation energy for both sorts of reactions by use of a single relation, as it is the case for the other empirical rules. Although the reason for this discrepancy is not yet clear, the following fact may tell us that at least a part of the inaccuracy attached to the present method is due to the lack of accuracy of the Rydberg's equation for large internuclear distances. Thus, for the activation energy of reaction No. 1 in Table 1:

$$H+p-H_2\rightarrow o-H_2+H,$$

Morse's equation gives 14.6 kcal. and Rydberg's equation gives 10.1 kcal. While from the potential-energy curve directly constructed by the use of the spectroscopic data we obtain 7.5 kcal., which agrees very well with the experimental value 7 kcal.

Geometrical Dimensions of Activated Complex

According to the present method of calculation the total length of the activated complex of the type X...Y...Z is given by the sum of the activated distances r^*_{XY} and r^*_{YZ}, since the form of this sort of complex must be linear. When we compare the values so calculated of X...Y, Y...Z and X...Y...Z with those calculated by means of the semi-empirical method of Eyring, we find an interesting result, namely, that the total length of the activated complex calculated according to both methods agree very well whereas the respective distances X...Y and Y...Z in the complex sometimes show remarkable differences between two methods, as is shown in Table 3.

Table 3

Dimensions of Activated Complex of Some Triatomic Reactions

Activated complex X...Y...Z	Length of X...Y, Å.		Length of Y...Z, Å.		Length of complex X...Y...Z, Å.	
	i	ii	i	ii	i	ii
H ...H ...H	1.12	0.75	1.12	1.35	2.24	2.10
H ...Br...H	1.80	1.40	1.80	2.10	3.60	3.50
Br...H ...H	1.80	1.42	1.12	1.50	2.92	2.92
H ...Cl...H	1.65	1.33	1.65	2.10	3.30	3.43
Cl...H ...H	1.65	1.30	1.12	1.40	2.77	2.70
H ...H ...Na	1.12	1.69*	2.55	1.94*	3.67	3.63*
H ...H ...K	1.12	1.84*	2.99	2.29*	4.11	4.13*

i, the present method. ii, the semi-empirical method.

* S. Shida and K. Nakata, the 2nd meeting of the Chemical Society of Japan, April 2, 1949.

Furthermore, as the constant a in Rydberg's equation does not vary so much from bond to bond and its mean value becomes 2.69 Å.$^{-1}$, we can roughly put

$$r^* = r_e + 1/a$$
$$= r_e + 0.37 \text{ Å}.$$

So it may be said that the average length of a bond in an activated complex is about 0.37 Å. longer than the equlibrium bond-distance.

Length of Hydrogen Bond

The present method of calculation gives us some interesting information on the length of the hydrogen bond. If we assume, namely, the hydrogen bond of the type R—X...H...Y—R′ as a sort of an activated complex of the reaction

$$\text{R-X-H} + \text{Y-R}' \rightarrow \text{R-X} + \text{H-Y-R}'$$

the length of the activated complex X...H...Y of the reaction

$$\text{X-H} + \text{Y} \rightarrow \text{X} + \text{H-Y}$$

may give at least the lower limit of the distance between X and Y in the above-mentioned hydrogen bond, because the bond energies of the diatomic molecules X—H and H—Y will appreciably be greater than those of RX—H and H—YR, so that the activated distances of the former will be shorter than those of the latter. This expectation was found actually the case as shown in Fig. 2, except for F...H...F, in which, however, our calculated value 2.38 Å. agrees fairly well with the value 2.32 Å. calculated by Pauling.[4]

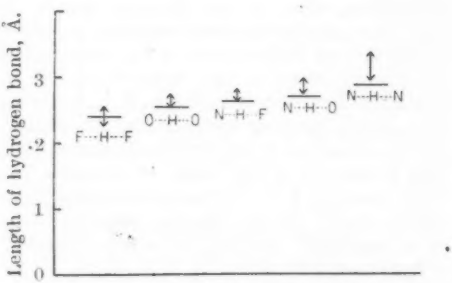

Fig. 2.—Length of the hydrogen bond.

Dissociated Adsorption of Hydrogen on Charcoal

As an example for the application of the present method to the heterogeneous reaction, we may cite the calculation of the activation energy for the dissociated adsorption of hydrogen on the surface of charcoal:

The activation energy calculated by means of the present method as a function of the C—C distance is plotted in Fig. 3 and compared with that of Sherman and Eyring,[5] who

(4) L. Pauling, "The Nature of Chemical Bonds", Cornell University Press, New York, 1940, p. 297.

(5) A. Sherman and H. Eyring, *J. Am. Chem. Soc.*, **54**, 2661 (1932).

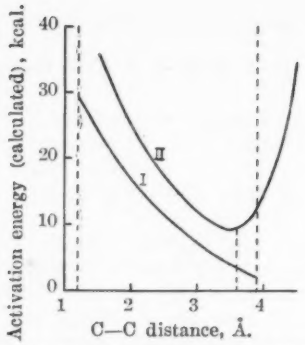

Fig. 3.—Activation energy of the dissociated adsorption of hydrogen on charcoal: I, by the present author; II, by Sherman and Eyring.

calculated the same energy by the use of the semiempirical method of Eyring putting $\rho=10$ %. The most favorable C—C distance for the adsorption, that is the distance, where the activation energy becomes mininum according to the present method, is 3.92 Å. corresponding to the structure of the linear form of the activated complex C...H...H...C, while this energy becomes minimum at the distance 3.6 Å. according to the semi-empirical method. But it may be worth while to mention that both curves in Fig. 3 coincide completely if the value of ρ in the calculations according to the semi-empirical method is taken somewhat larger than 10%.

Summary

1. It has been assumed that the bond-distance in an activated complex is equal to the bond-distance corresponding to the inflexion point on the potential-energy curve of the pair of atoms.

2. According to this fundemental assumption, a new simple method of calculation of activation energy of reactions has been devised.

3. The method has been applied to some kinds of triatomic reactions and the double decompositions between two diatomic molecules with satisfactory results.

4. For the triatomic reactions, the geometrical length of the activated complexes computed by means of the present method agrees well with those calculated by means of the semi-empirical method of Eyring.

5. It has been shown that the present method of calculation gives some information on the lower limit of the length of the hydrogen bond.

6. The activation energy for the dissociated adsorption of hydrogen on the surface of charcoal has been calculated as a function of the distance between two carbon atoms. The result obtained agrees well with that obtained by Sherman and Eyring according to the semi-empirical method.

The author wishes to express his sincere thanks to Prof. T. Titani for his interest in this research. The author is also indebted to Dr. T. Horie for his kind information on the spectroscopic data.

Faculty of Science, Osaka University, Osaka

The Electrical Conductivity of the Condensed Polynuclear Aromatic Compounds

By Hiroo Inokuchi

(Received June 12, 1951)

Introduction

In the previous paper,[1] the electrical conductivity of violanthrone, isoviolanthrone and pyranthrone has been reported. These substances belong to the condensed polynuclear aromatic compound. The electrical conductivity of these substances has been attributed to π-electrons of the conjugated double bonds of network-plane of carbon atoms. The highest limit of this network-plane is graphite, which has the electrical resistivity of $10^{-3}\,\Omega$cm. (powdered state). On the other hand, the electrical resistivity of benzene, the lowest limit of these substances, is higher than $10^{18}\,\Omega$cm.

(1) H. Akamatu and H. Inokuchi, *J. Chem. Phys.*, **18**, 810 (1950).

in the solid state. Therefore the electrical conductivity of these compounds in the solid state are closely corelated to the numbers of rings which are contained in the network-planes, and also to the π-electrons of these molecules. From this standpoint, the study has been extended over a series of compounds belonging to this group.

Experimental Procedure

Because the single crystals could not be obtained, eleven samples of this group, described below, were examined in the state of compressed powdered form. For the higher conductive substances, the method has been already described, apparatus-I, which was like that used by Brunner and Hammerschmid for measuring the conductivity of powdered graphite.[1],[2],[3] In this method, the specimen was compressed between the metal end and piston in the polished ebonite cylinder of good quality or ambroide cylinder, and the electrical resistivity was measured by the potential drop method with the aid of direct current amplifier.

For the lower conductive substances, another apparatus was used (Fig. 1: apparatus-II). The specimen was compressed on a cylindrical dish, which was made of brass coated by chromium, by a piston to 80 kg./cm.^{2} with a lever system. This piston was insulated by ambroide (1) (5) and pyrex glass (4). The electrical resistivity observed depends, in the first approximation, on the area of the end of the piston, which is 0.503 cm.^{2}. This apparatus has an advantage over the former in regard to the problem of the effects of the temperature and surface leakage. The surface leakage could be avoided and the temperature could be increased to 300°, because the ebonite cylinder was not used.

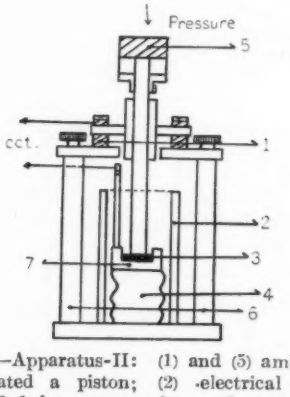

Fig. 1.—Apparatus-II: (1) and (5) ambroide insulated a piston; (2) electrical oven, shielded by copper plate; (3) specimen; (4) pyrex glass; (6) brass; (7) cylindrical dish, coated by chromium.

In the previous paper,[1] it was found that in each case the constancy of the electrical conductivity of these powdered specimens is obtained when the compressed pressure upon them is over 80 kg./cm.^{2}. This fact was supported again in the following manner.

The electrical conductivity of anthanthrene ($C_{22}H_{12}$: m. p. 257.5°-258°) was measured by the apparatus-II under 80 kg./cm.^{2} pressure. The temperature was increased to 264°, above the melting point of this crystal, and then decreased to the room-temperature. The hysteresis of electrical conductivity upon the increasing and decreasing of temperature was almost negligible (Fig. 2). This fact shows that the contact resistance between the powdered crystals was not affected practically under 80 kg./cm.^{2} or more in pressure. Therefore, the value of electrical conductivity measured by these methods was assumed to be intrinsic.

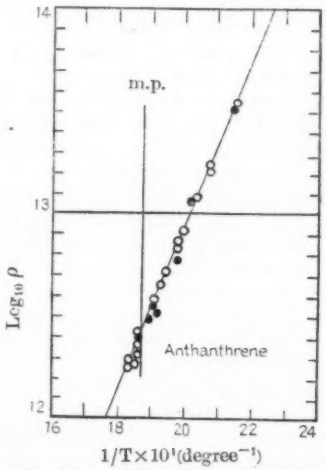

Fig. 2.—The relation between resistivity and temperature for anthanthrene by the apparatus-II: ○ 80 kg./cm.^{2}, before melted; ● 80 kg./cm.^{2}, after melted.

The samples were purified chemically[4] and then sublimed in vacuum (10^{-2}-10^{-5} mm. Hg.) more than two times until the conductivity was constant. The vacuum sublimation is an extremely advantageous method; the impurities—starting substances, by-products and carbonious matters etc.—were completely separated in the manner just like chromatography, and also there was no trace of solvent between crystals at all.

(2) H. Akamatu and H. Inokuchi, *J. Chem. Soc. Japan*, **70**, 185 (1949).

(3) J. Brunner and H. Hammerschmid, *Z. Electrochem.*, **40**, 60 (1934).

(4) H. Akamatu and K. Nagamatsu, *J. Colloid Sci.*, **2**, 593 (1947).

Table 1

The Value of ρ_{15}, $\Delta\xi$ and ρ_0 of the Condensed Polynuclear Aromatic Compounds.

No.	Substance	Structure	ρ_{15}, Ωcm.	$\Delta\xi$, e. V.	ρ_0, Ωcm.
1	Isoviolanthrone	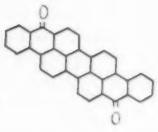	5.7×10^{9}	0.75	1.5×10^{3}
2	Isoviolanthrene	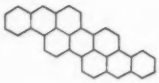	8.4×10^{13}	0.82	6.3×10^{6}
3	Violanthrone	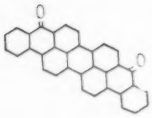	2.3×10^{10}	0.78	2.9×10^{3}
4	Violanthrene	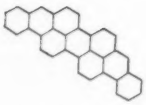	2.1×10^{14}	0.85	6.85×10^{6}
5	Ovalene		2.3×10^{15}	1.13	3.1×10^{5}
6	Pyranthrone	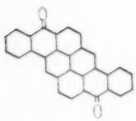	3.9×10^{15}	1.06	3.7×10^{6}
7	Pyranthrene	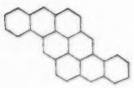	4.5×10^{16}	1.07	2.0×10^{7}
8	Meso-naphthodianthrone		1.5×10^{18}	1.30	6.0×10^{6}
9	Meso-naphthodianthrene		4.0×10^{18}	1.2	1.8×10^{5}
10	Anthanthrone	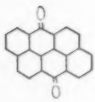	7.7×10^{18}	1.70	9.7×10^{3}
11	Anthanthrene		1.5×10^{19}	1.67	3.4×10^{4}

Results and Discussion

The names and colours of solid specimens used are;

(1) isoviolanthrone (dark green), (2) isoviolanthrene (red), (3) violanthrone (violet), (4) violanthrene (dark red), (5) ovalene (reddish-orange), (6) pyranthrone (orange-red), (7) pyranthrene(brown), (8) meso-naphthodianthrone (greenish-yellow), (9) meso-naphthodianthrene (dark green), (10) anthanthrone (scarlet) and (11) anthanthrene (brownish-yellow). Their molecular structures were illustrated in Table 1.

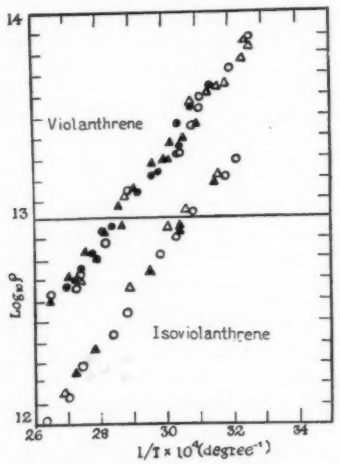

Fig. 3a.—The relation between resistivity and temperature for violanthrene and isoviolanthrene by the apparatus-I: △ 82.1 kg./cm.², rising temperature; ▲ 82.1 kg./cm.², falling temperature; ○ 119.5 kg./cm.², rising temperature; ● 119.5 kg./cm.², falling temperature.

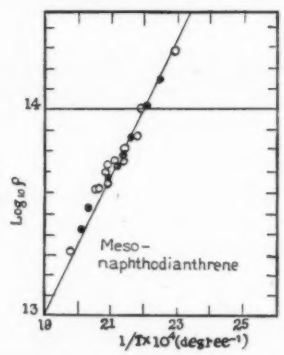

Fig. 3b.—The relation between resistivity and temperature for meso-naphthodianthrene (apparatus-II): ○ 80 kg./cm.², rising temperature; ● 80 kg./cm.², falling temperature.

The logarithm of electrical resistivity $\log \rho$ and the reciprocal of temperature $1/T$ have the linear relation as in the case of violanthrone etc.,

$$\rho = \rho_0 \exp(\Delta\epsilon / 2kT). \qquad (1)$$

Some examples of this relation are illustrated on Figs. 2 and 3. The value of ρ_0, ρ at 15° (extrapolated value), and $\Delta\epsilon$ are shown in Table 1.

The good reproducibility of electrical resistivity against temperature, non-effect from the moisture and independency of the current upon the time proved the electronic conduction.

We think these substances to be the electronic semi-conductor from the characteristics of Eq. (1), and this assumption is also supported by the fact that violanthrone and violanthrene, for example, have the sensitive photoconductivity which is now under investigation. As these organic compounds are prefect molecular crystals, we cannot consider the possibility of impurity-level such as in the cases of CuS or PbS.

For these reasons they must be intrinsic semi-conductors. In Table 1 it is found that the electrical conductivity is increased together with the numbers of π-electron or the conjugated double bonds in molecule, and $\Delta\epsilon$, corresponding to the energy difference between the empty level and the occupied level of the crystal on the model of semi-conductors, is decreased with the increasing of the numbers of π-electron in the molecule.

To confirm the contribution of π-electron to the electrical conductance, the conductivity of Hydro-violanthrene (yellow), which was made by the strong reduction from violanthrone by the red phosphorus and hydrogen iodide, was measured by the apparatus-II. The numbers of the π-electron of this substance are decreased by the strong reduction illustrated as Fig. 4, and also the mobility of electrons will be restricted in the molecule. The measurement was carried out under 80 kg./cm.² in pressure and heated above 250°, over the melting point of this compound.

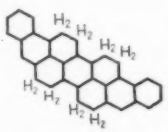

Fig. 4.—The structure of hydro-violanthrene.

Compared with the other compounds, the result of temperature-resistivity relation was

the same, Fig. 5, but the difference of energy band, $\Delta\epsilon$, and extrapolated resistivity to 15°, ρ_{18}, have exceedingly higher value. These results were tabulated on Table 2 with violanthrone and violanthrene. It is shown by this result that the existence of π-electrons in these substances leads to electrical conductance.

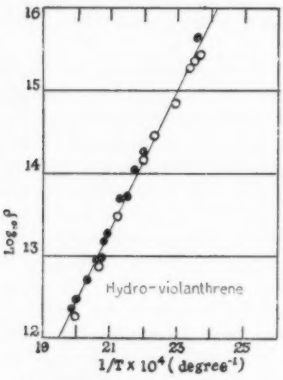

Fig. 5.—The relation between resistivity and temperature for hydro-violanthrene: the same symbols as in Fig. 3b.

Table 2

The Value of ρ_{15}, ρ_0 and $\Delta\epsilon$ of Hydro-violanthrene, Violanthrene and Violanthrone.

	Hydro-vilanthrene	Violanthrene	Violanthrone
Colour	yellow	dark red	violet
ρ_{15}, Ωcm.	1.1×10^{25}	2.1×10^{14}	2.3×10^{10}
ρ_0, Ωcm.	3.0×10^{-5}	6.85×10^{6}	2.9×10^{3}
$\Delta\epsilon$, e. V.	3.4	0.85	0.78

The quinonoid structures of this group lead to a great increase of electrical conductivity as compared with its hydrocarbons, but the intervals of energy band, $\Delta\epsilon$, have the same value. And in comparsion with the magnetic susceptibility of this group, it is interesting to note that the electrical conductivity was not affected greatly by the shape of the molecule, but by the numbers of π-electron alone.

Summary

The electrical conductivity of the condensed polynuclear aromatic compounds; (1) isoviolanthrone, (2) isoviolanthrene, (3) violanthrone, (4) violanthrene, (5) ovalene, (6) pyranthrone, (7) pyranthrene, (8) meso-naphthodianthrone, (9) meso-naphthodianthrene, (10) anthanthrone and (11) anthanthrene,—has the character of a semi-conductor. The resistivity of these compounds can be expressed as $\rho=\rho_0 \exp(\Delta\epsilon/2kT)$. The value of $\Delta\epsilon$ and ρ at 15° were found as, (1) 0.75 e. V., 5.7×10^{9} Ωcm., (2) 0.82 e. V., 8.4×10^{13} Ωcm., (3) 0.78 e. V., 2.3×10^{10} Ωcm., (4) 0.85 e. V., 2.1×10^{14} Ωcm., (5) 1.13 e. V., 2.3×10^{15} Ωcm., (6) 1.06 e. V., 3.9×10^{15} Ωcm., (7) 1.07 e. V., 4.5×10^{16} Ωcm., (8) 1.30 e. V., 1.5×10^{18} Ωcm., (9) 1.2 e. V., 4.0×10^{18} Ωcm., (10) 1.70 e. V., 7.7×10^{18} Ωcm., (11) 1.67 e. V., 1.5×10^{19} Ωcm.. The good reproducibility and non-hysteresis of the electrical conductivity for temperature suggests electronic conduction. As these organic compounds have a perfect molecular lattice, the possibility of impurity-level cannot be considered. For this reason the mechanism of the conduction is assumed to be that of the intrinsic semi-conductor.

The author expresses hearty thanks to Prof. H. Akamatu for his kind direction in this work and also to Mr. T. Handa who prepared most of the samples of this work, especially the synthesis of ovalene was due to his effort. The cost of this research has been defrayed from the Scientific Research Encouragement Grant from the Minstry of Education to Prof. H. Akamatu, to which the author's thanks are due.

Chemical Department, Faculty of Science the University of Tokyo, Tokyo

So-called Silica Content of Natural Waters

Iwaji IWASAKI, Takashi KATSURA and Toshikazu TARUTANI

(Received June 12, 1951)

After the work of Dienert and Wandenbulcke[1], many workers have given various analytical methods for the determination of silica in natural waters and have discussed the state of silica. It is probable that various kinds of silicon compounds, such as soluble silica and silicate, colloidal silica, silicates, organic substances (biological materials) containing silicon or silica, etc., exist in natural waters, especially in river waters. Practically, it is very difficult to distinguish these silicon compounds respectively. So we use, for convenience sake, the word silica instead of silicon compounds in this paper.

Silica in natural waters is mainly determined by colorimetric methods, but it is doubtful that the value obtained by the colorimetric method shows the total silica content. It seems that silica obtained by colorimetry is in ionic form and not in colloidal state[1]. After the treatment with alkali bicarbonate or carbonate solution, so-called colloidal silica is also considered to produce a yellow color similar to that developed by the compounds in ionic form treated by the same method. On contrary, very small particles of colloidal silicates and quartz, etc., in the waters can not be determined by the colorimetric method, unless these compounds are converted into soluble silicate by fusion with alkali carbonate or hydroxide. (Compare with the suggestive investigations of W. Noll[2], F. W. Correns,[3] etc.).

On the other hand, A. R. Tourkey[4] thought that silica obtained by colorimetric method is mainly colloidal. C. J. Roy[5] stated that in natural waters silica is actually present in the form of acid ions and not in the colloidal state.

We had a doubt concerning these conclusions described above, and have carried out the following experiments to ascertain the real facts.

(1) F. Dienert and F. Wandenbulcke, *Compt. rend.*, **176**, 1478 (1923).
(2) W. Noll, *Chem. der Erde*, **6**, 1 (1931).
(3) C. W. Correns, *Chem. der Erde*, **13**, 92 (1940); *etc.*
(4) A. R. Tourkey and D. H. Bangam, *Nature*, **138**, 584 (1936).
(5) C. J. Roy, *Am. Jour. Sci.*, **243**, 393 (1945).

Experiments

Colloidal Silica in the Mineral Water of Shiroike Hot Spring at Beppu, Oita Prefecture.—The spouting water of Shiroike Hot Spring is colorless and transparent, its temperature is 99°, and the pool water of Shiroike Hot Spring is milky white. Both spouting water and pool water are nearly neutral and the silica contents of these mineral waters show the same value by gravimetric method. The chemical composition of the mineral water of Shiroike Hot Spring is shown in Table 1.

Table 1

	Spouting water		Pool water	
	Sept., 1949	March, 1950	Sept., 1949	March, 1950
Evaporated residue	5.052g./l.	5.045g./l.	5.227g./l.	5.348g./l.
SiO_2	0.559	0.572	0.537	0.529
CaO	0.146	0.244	0.154	0.196
MgO	trace	trace	trace	trace
Cl	—	2.383	—	2.539
SO_4	—	0.235	—	0.263
Alkali halide	3.941	3.642	3.575	3.963
*p*H	7.6	7.4	7.8	7.4

The value of silica content of pool water obtained by colorimetric method is very small compared with that by gravimetric method. From the results of electrodialysis and gravimetric analysis, we found that the pool water contains a considerable quantity of colloidal silica. In the spouting water immediately after sampling, the silica content obtained by colorimetric method is the same as that obtained by gravimetric method, but after sampling, as time goes on, the value of the silica content obtained by colorimetric method decreases until the constant value is reached (Table 2). We found the same phenomena in sodium silicate solution, and Aoki[6] found the same fact independently. More detailed reports will be published elsewhere.

(6) F. Aoki, *J. Chem. Soc. Japan*, **72**, 15 (1951).

Table 2

March, 1950 A		March, 1950 A		Sept., 1949 B		Sept., 1949 C[3]		July, 1947 D	
Time[1]	SiO_2 mg./l.[2]	Time	SiO_2 mg./l.[2]	Time	SiO_2 mg./l.[2]	Time	SiO_2 mg./l.[2]	Time	SiO_2 mg./l.[2]
15 min.	640	15 min.	640	5 days	250	0	366	436 days	128
30	455	1 days	145	7	225	15 min.	343	586	114
45	310	2	140	8	193	30	338		
1 hr.	310	3	138	15	130	40	329		
2	242	4	139	19	126	4 hr.	236		
5.5	153	5	133	160	125	26	149		
22	145	6	100						
48	140	10	101						

1) The time measured from sampling.
2) Value obtained colorimetric method.
3) The sample is the aged sample of 5 days from sampling. (Sample B, SiO_2=250 mg./l.). Measurements are started after boiling for 3 minutes.

We transferred a 100 cc. spouting water into a platinum dish (the silica content of this spouting water reached the constant value by colorimetry.), and added 0.4 g. of sodium bicarbonate in it, and heated it on a boiling water-bath for an hour. We found that the silica content of the aged spouting water treated with sodium bicarbonate found by colorimetry is the same value as that by gravimetric method. Next we tried the electrodialysis of aged spouting water which showed the constant silica content by colorimetry to ascertain the existence of colloidal silica and could obtain colloidal silica. We used in this case cellophane membrane having the pore size of 2-3 mμ measured with dyes.

Colloidal silica in residual water produced no color with ammonium molybdate by the usual colorimetric method, but after treatment with sodium bicarbonate, the silica content obtained by colorimetry is the same as that by gravimetric method (Table 3).

Table 3

	I	II	III	IV
Spouting water	0.559g./l.	0.130g./l.	0.223g./l.	0.222g./l.
Pool water	0.537	0.116	0.338	0.336

I. Total SiO_2 (With gravimetry).
II. SiO_2 reached constant value (Colorimatry).
III. Residual SiO_2 after dialysis (Gravimetry).
IV. SiO_2 treated with sodium bicarbonate of residual sample after dialysis (Colorimetry).

From these results of experiments, we could show that colloidal silica is actually present in the mineral water of Shiroike Hot Spring and colloidal silica having a larger particle size than about 2-3 mμ can not produce the yellow color by ammonium molybdate in acidic solution. The loss of silica content obtained by colorimetry as time goes on after sampling is considered to be due to the fact that ionic silica is coagulated and produces colloidal silica.

Various Kinds of Silicon Compounds in River Water and Japanese Standard Sea Water.—In order to ascertain the presence of various kinds of silicon compounds in natural waters, we have carried out experiments according to the following four different methods for the colorimetric determination of silica.

Method 1. (Usual colorimetric method). To 20 cc. of sample solution are added 2 drops of sulfuric acid (1:1) and 0.5 cc. of 10% ammonium molybdate solution, and the yellow color developed is compared after about ten minutes with that of the standard solution (picric acid and potassium chromate solution). By this method soluble silica and silicate are determined.

Method 2. (Colorimetric method after treatment with sodium bicarbonate). To 50 cc. of sample solution is added 0.2 g. of sodium bicarbonate in a platinum dish, the mixture is heated on a boiling water bath for an hour. Then it is cooled and neutralized with sulfuric acid (1:1) and diluted with water to 50 cc. Colorimetric determination of silica in the solution thus obtained is carried out as the method 1.

Method 3. (Colorimetric determination of silica after treatment with sodium carbonate). In this method, 0.5 g. of sodium carbonate is used instead of sodium bicarbonate. All other procedures are the same as the methods 1 and 2 described above.

By the methods 2 and 3, soluble silica, soluble silicate, so-called colloidal silica, etc. are determined.

Method 4. (Colorimetric determination of silica after carbonate fusion). 20 cc. of sample solution is gently evaporated up to dryness in a platinum crucible, and the residue is covered with about 1 g. of anhydrous sodium carbonate, and then the crucible is heated over a small flame, and the mixture is fused for a further 10 minutes. The crucible is allowed to cool down. After the

crucible has cooled down completely it is filled with water to 2/3 of its height and its bottom is gently heated. The melted substance is treated with water, and then the *p*H-value of the solution thus obtained is adjusted to about 1.4 by means of diluted sulfuric acid (1:1) and 1 cc. of 10% solution of ammonium molybdate is added. The colorimetric method after this treatment is the same as the usual method. By this method, all silicon compounds are determined.

By these analytical methods we can distinguish various silicon compounds in natural waters from each other. For example, the silica content of the water of Tamagawa river, flowing into the Bay of Tokyo, is shown in Tables 4 and 5. Silica content in Table 4 was determined by gravimetric method and in Table 5 by colorimetric method described above.

Table 4

	mg./l.
Evaporated residue (110°C.)	155
Si	41.4
Al	5.8
Fe	0.18
Ca	15.6
Mg	1.8
Na	6.6
K	0.8
Mn	0.032
Cl	12
*p*H	6.4

Table 5

Silicon Content of the River Water of Tamagawa

Date	Method 1	Method 2	Method 3	Method 4
	mg./l.	mg./l.	mg./l.	mg./l.
9, August	20.0	—	—	—
10, 〃	20.0	21.4	—	44.5
11, 〃	19.5	20.5	20.3	—
13, 〃	18.5	20.7	20.9	35.4
14, 〃	15.8	—	20.2	24.3

As seen in Tables 4 and 5, as time goes on after sampling, the silica content of river water in the sample bottles decreases owing to deposition of dispersed particles in the waters.

As seen in Table 5, the silica content obtained by method 1 is the smallest and that by method 4 is the greatest among them. The silica content obtained by method 2 is almost the same as that by method 3.

From these results we concluded that there are various kinds of silicon compounds in the water of Tamagawa river in addition to the soluble silica and silicates.

In Table 6, similar results obtained on Japanese standard sea water are shown.

Table 6

Silicon Content of the Japanese Standard Sea Water

	Method 1	Method 2	Method 3	Method 4
	mg./l.	mg./l.		mg./l.
Sample No. 1	4.1	4.5	—	—
Sample No. 2	4.0	—	—	6.8

As seen in Table 6, these values are too high compared with that of J. Robinson's and Wattenberg's values. In the other experiments of sea water, however, the silica content of sea water at, for example, Fukuoka, or Enoshima is lower than that described above.

We also observed that the yellow color of the sea water at Hakozaki, Fukuoka City, produced by ammonium molybdate after treatment with sodium bicarbonate is remarkably deeper than that developed by method 1.

The silica content of the sea water containing cultivated diatom is measured by the methods described above, and the results obtained are shown in Table 7.

The silica content of the sea water containing cultivated diatom is 20.7 mg. SiO_2/l. by gravimetric method, and the same value was obtained by method 4. As seen in Table 7, most of the silica in this sample does not produce yellow color by method 1. The silica content of sample 1, obtained by method 2 is greater than that given by method 1, but less than that by method 4. However, in the cases of samples 2 and 3 which are diluted to double volume with distilled water before treatment, there is no difference between the value obtained by method 2 and that by method 4.

Table 7

	Method 1	Method 2	Method 3	Method 4
	mg./l.	mg./l.		mg./l.
Sample No. 1	<1.0	8.6	—	20.7
Sample No. 2	<1.0	10.6	—	10.6
Sample No. 3	<1.0	10.6	—	11.0

Conclusions

From the results obtained above, we reached the following conclusions.

1. Colloidal silica is actually present in natural waters such as Shiroike Hot Springs, the Tamagawa river, etc.

2. Colloidal silica, which has a diameter larger than 2–3 mμ, does not produce yellow

colour with ammonium molybdate in the acidic solution.

3. As ionic silica is coagulated and produces colloidal silica in natural waters, colorimetry for the determination of silica must be performed immediately after sampling. The silica content of an aged sample by method 1 is frequently remarkably less than that obtained from a fresh sample.

4. As colloidal silica can not be determined by method 1, even if it is present, methods 2, 3, and 4 must be used for the determination of silica content.

5. Various kinds of silicon compounds are actually present in natural waters, such as the Tamagawa river, etc.

6. In many cases, the total silica contents of natural waters are obtained by methods 2, and 3, but for the determination of the total silicon in natural waters method 4 must be used.

The authors express their heartly thanks to Mr. K. Tachibana, Faculty of Science, Kyushu University, and Professor Y. Matsue and Mr. A. Saeki, Faculty of Agriculture, Tokyo University, for their helpful advice and sincere friendship which facilitated this work.

The cost of this research was defrayed from the Scientific Research Encouragement Grant from the Ministry of Education, to which the authors wish to express their thanks.

Laboratory of Analytical Chemistry and Geochemistry
Tokyo Institute of Technology, Tokyo

Physicochemical Properties of the Surface of Aqueous Solutions. II. Foam Stability and Mechanical Properties of Surface

By Hideo KIMIZUKA and Tunetaka SASAKI

(Received June 13, 1951)

Introduction

It has been generally accepted that the viscoelastic properties of the surface of a solution has an intimate relation to the various phenomena occurring in them such as the foam or the emulsion formation.(1) In these relations, we have already studied the foam of saponin solution, especially in connection with the surface tension, the membrane effect and the semiquantitative measurement of the surface viscosity of the aqueous solution.(2),(3) In the present paper the results of further experiments on these lines are described.

Apparatus and Method

Up to the present, various methods have been employed for the measurement of the surface viscosity.(1),(4) In the present study, however, a new and simple apparatus was employed as shown in Fig. 1a. In this figure AB shows a fine thread of glass with the diameter of 0.02 cm. and the length of 30 cm., of which one end (B) is fused to a firm glass rod support, while a platinum wire with horizontal part CC′ of 1 cm. in length as shown in Fig. 1b is fixed to the other end (A). Again in Fig. 1a, D is a shallow glass vessel with the diameter of 6 cm. and the depth of 1.5 cm., in which a solution for measurement is introduced. E is a table, carrying the vessel on it and is able to move vertically by means of a screw.

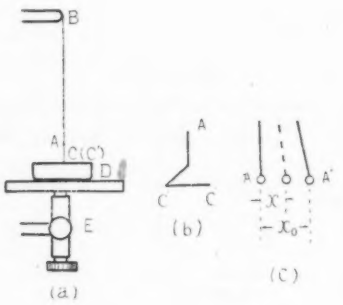

Fig. 1.—Surface viscometer.

(1) R. E. Wilson and E. D. Ries, "*Colloid Symposium Monograph*," **1**, 145 (1923); D. Talmud, S. Suchowolskaja and L. Lubman, *Z. Physik. Chem.*, **A 151**, 401 (1930); etc.

(2) T. Sasaki, This Bulletin, **15**, 449 (1940); T. Sasaki and S. Mitui, *ibid.*, **18**, 259 (1943).

(3) H. Kimizuka and T. Sasaki, *Mem. Fac. Sci., Kyûsyû University, Ser. C*, **1**, 197 (1950); T. Sasaki, unpublished.

(4) L. Fourt and W. D. Harkins, *J. Phys. Chem.*, **42**, 897 (1938); E. R. Washburn and H. R. R. Wakeham, *J. Am. Chem. Soc.*, **60**, 1294 (1938); L. Fourt, *J. Phys. Chem.*, **43**, 887 (1939).

The measurement of the surface viscosity is carried out as follows. Platinum wire CC′ is first forced to shift from the rest position A (in the air), fixed by a suitable device to a certain position A′ as shown in Fig. 1c, and the distance between A and A′ is measured. Then the surface of solution is carefully forced up untill it just touches the platinum wire at A′. After a desired time of aging of the surface, the platinum wire is set free and allowed to return from A′ to A under the action of force chiefly exerted by the elasticity of glass thread. Now the successive measurements of the position of platinum wire and accordingly the distance X from A is measured with the time t. When we plot $\ln X$ against t is plotted, and a linear relation can be obtained, as follows;

$$\ln X = \ln X_0 - kt. \qquad (1)$$

Differentiating Eq. (1) with respect to time, an equation of the form can be gained:

$$l\frac{dx}{dt} + mx = 0,$$

where

$$k = m/l. \qquad (2)$$

Eq. (2) means that the motion of platinum wire is governed by two forces: namely a restoring force mx, proportional to the deflection of glass thread, and a viscous resistance $l\ dx/dt$, proportional to the velocity of platinum wire, mainly exerted by the surface of a solution. Consequently, m is a constant relating to the elasticity of glass thread, and l is a measure of surface viscosity. Since m is known ($m=2.16\times10^{-3}$ dynes/cm.), the relative surface viscosity coefficient l can be calculated according to Eq. (2). It can be noted here, that a lack of a constant term in Eq. (2) is an indication of the absence of surface elasticity. For carrying out the experiment, the initial displacement given to the platinum wire, x_0, is kept constant to 0.2 cm., and x is measured by means of a comparator to the accuracy of 10^{-3} mm. Whole apparatus is set in a large glass vessel to keep it free from the occasional contamination such as dust.

The surface tension was measured by means of du Noüy's tensiometer and a capillarimeter. The membrane effect was also measured which was expressed by the difference between the apparent surface tension calculated from the capillary rise under the condition of receding and advancing menisci.[3]

For the measurement of the foam formation, 10 cc. of solution is introduced in a well stoppered test tube of 1.5 cm. in diameter and 17 cm. in length, and is shaken fifty times for ten seconds with an amplitude of 12 cm. After shaking, the height of the foam zone (h) produced just after the stop of shaking and the time (τ) required for the foam to breakdown into half of its initial volume were measured.

Samples used were the commercial one and were not purified further. Water used for the preparation of the solution is freshly distilled. The experiments were carried out at room temperature.

Results of Experiments

In order to visualize the surface viscosity of a certain solution, a series of experiments was carried out which is shown in Table 1. Accuracy of the value l is ±0.01 g./sec.

Table 1

Sample	Experimental condition	Time of aging, hr.	Surface viscosity l, g./sec.
Water	Pt wire touching a surface	0	0.00
	〃	5	0.00
	Pt wire dipping in water	5	0.00
Saponin solution (0.030 g./l.)	Pt wire touching a surface	5	0.60
	Pt wire dipping in solution	5	0.00

The results of measurements of the surface tension σ, surface viscosity l, foam height h and life of foam τ are shown in Fig. 2 where l and σ are the values referred to a solution surface aged for one hour. In Fig. 2 the ordinate represents the substances under investigation where the numbers in brackets indicate the concentration (in percentage) of solutions employed, and the abscissa, τ, h, σ and l.

The measurements of the surface viscosity, surface tension, height of foam, life of foam and membrane effect were also carried out with the saponin~ethyl alcohol~water system containing a fixed amount of saponin (0.030 g./l.) and varying amount of ethyl alcohol. These values were plotted against the logarithm of concentration in mol./l. of ethyl alcohol as shown in Fig. 3, where the values of the surface viscosity and surface tension are those

Table 2

Effect of Electrolyte on the Life and Height of Foam of Saponin Solution (0.030 g./l.)

Electrolyte	Concentration, N	pH	Surface viscosity l, g./sec.	Life of foam τ, hr.	Height of foam h, cm.
—	0	5.9	0.10	0.5	1.2
HCl	1×10^{-2}	2.0	0.10	0.5	1.2
KCl	5×10^{-1}	5.9	15.0	4.0	1.2
$BaCl_2$	5×10^{-4}	5.9	145.	25	1.2
$AlCl_3$	3×10^{-5}	3.0	280.	26	1.2
$Th(NO_3)_4$	5×10^{-5}	2.0	350.	28	1.2

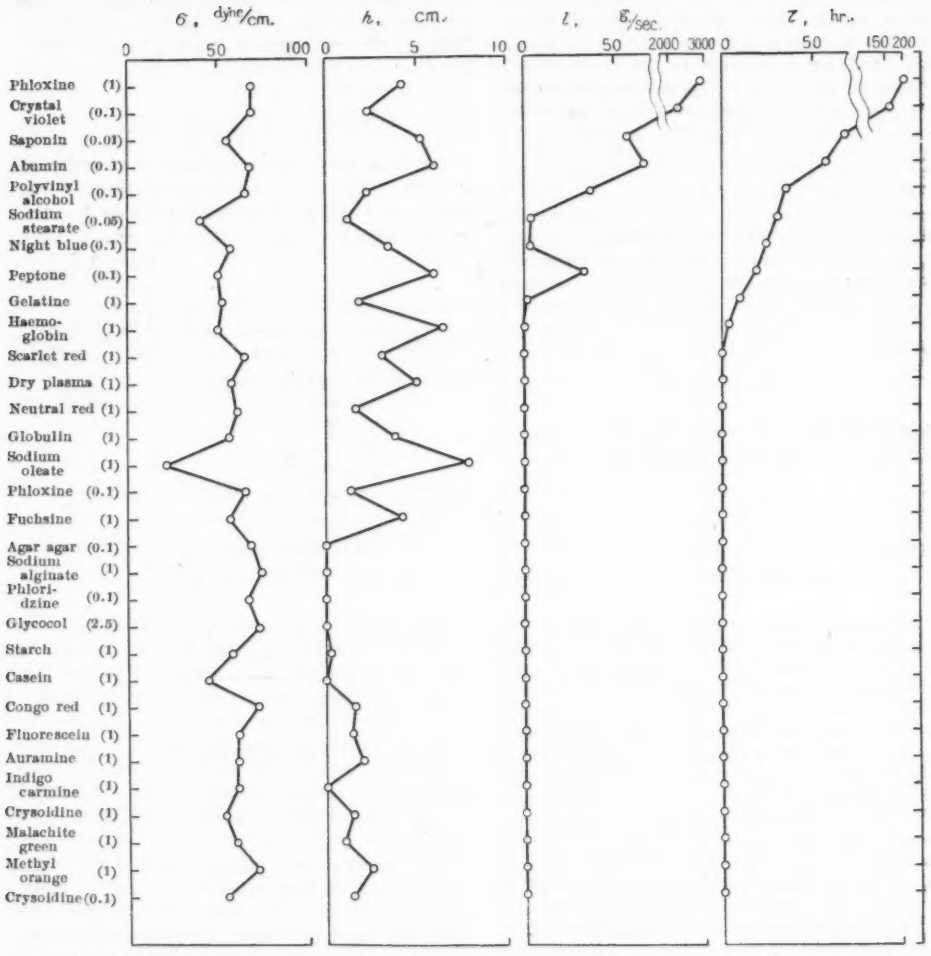

Fig. 2.—Surface tension σ, height of foam h, surface viscosity l and life of foam τ of solutions.

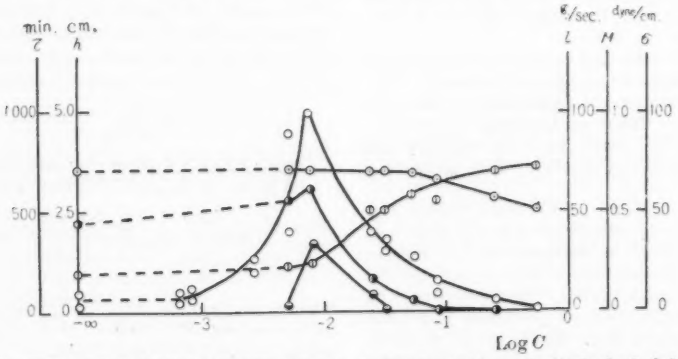

Fig. 3.—Saponin~ethyl alcohol~water system: C; concentration of ethyl alcohol in mol./l.; ○ life of foam, τ; ① height of foam, h; ◒ surface viscosity, l; ⊙ surface tension, σ; ◑ membrane effect, M.

of the solution surface aged for one hour. The similar measurements were also carried out for the saponin~electrolyte~water systems containing the fixed amount of saponin (0.030 g./l.) and varying amount of electrolyte. The results are tabulated in Table 2. Here *p*H was controlled by hydrochloric acid.

Discussion

As shown in Table 1, no appreciable amount of viscosity was susceptible by the present device in the surface and interior of distilled water, and also in the interior of many solutions. Consequently, it must be emphasized that the apparent viscosity frequently observed in the surface of aqueous solution is considered to be due to the surface only.

Many investigators have studied the formation of the coherent adsorbed layer in the surface of the aqueous solution. Wilson and Ries[1] showed qualitatively that the surface plasticity is parallel with the foam stability. Rehbinder[5] also reported a similar result. It can be seen in Fig. 2 that a close correlation can be found only between the surface viscosity and the life of foam, while no correlation between any other pairs of properties can be found. Wo. Ostwald[6] pointed out that the solutions of saponin, sodium stearate, night blue, gelatine, albumin and peptone which showed a remarkable membrane effect were capable of producing the extremely stable foam. These circumstances are just the same as in present experiment.

The result of measurements with the saponin~ethyl alcohol~water system is shown in Fig. 3, in which a distinct correlation between the membrane effect, the surface viscosity and the life of the foam can be found, *i. e.*, all these quantities exhibit sharp maxima at the same concentration of alcohol. The surface tension and the foam height, however, do not show a simple correlation to these quantities. Wo. Ostwald[6] made the measurements of the membrane effect and the foam height, and concluded that no direct correlation could be found between them. As discussed in the preceding paper,[3] however, the membrane effect can be interpreted as the measure of mechanical strength of surface layer, so it might well be considered to relate rather to the foam stability than to the foaminess or foam height as in the present experiment. The formation of such a stable coherent adsorbed layer by the addition of ethyl alcohol is considered to be due to its action of dehydration towards saponin with a subsequent promotion of the saponin adsorption to the surface. At a high concentration of alcohol, however, the life of foam again becomes almost zero resulting perhaps from the preferential adsorption of alcohol in the surface layer with the exclusion of saponin. This may also offer an explanation for the fact that the surface tension and the life of foam decrease rapidly at the same region of the concentration of alcohol.

In Table 2, the effect of electrolytes upon some properties of the aqueous saponin solution is shown. There we can see a marked valency effect of added cation even in high dilution upon the surface viscosity and the life of foam of the saponin solution. Cataphoretic behavior indicates that saponin is a negative colloid,[7] so that these effects may be explained as the coagulation of the adsorbed layer of saponin by electrolytes, which will be compared with the case of the stabilization of the gelatine foam by the added electrolytes studied by one of the present authors[8] and also with some other cases of the protein foam.[9],[10] In Table 2, it is also confirmed that the surface viscosity and the foam life are closely related to each other, while the height of foam shows no simple relation to both of them.

Further, the assumption in the preceding paper[3] that the membrane effect is not a phenomenon of the hysteresis of wetting, but is the indication of the formation of the coherent adsorbed layer and is therefore a measure of strength of surface film, is in good agreement with the experimental facts shown in Fig. 3. Recently Nakagaki[11] accounted for the foam formation of aqueous solutions of alcohols and several electrolytes assuming that the foam stability is closely related to the energy required to remove the unit area of adsorbed layer from the surface of the solution, thereby using the Gibbs' adsorption equation. But the systems studied in our experiment are those in which the surface tension changes irregularly with time, and frequently even an irreversible surface gelation takes place. Therefore Gibbs' adsorption equilibrium cannot be considered to hold in such a case. We should seek for some other factors to arrive at a more

(5) P. A. Rehbinder and A. A. Trapeznikov, *Comptes rends (Doklady) de l'Academie des Sciences d l' U. S. S. R.*, **18**, No. 7, 423 (1938); *ibid*, 427 (1938).

(6) Wo. Ostwald and A. Steiner, *Kolloid-Z.*, **36**, 342 (1925); Wo. Ostwald and M. Meiszner, *Kolloidchem.-Beih.*, **26**, 1 (1926).

(7) R. Ruyssen and R. Loos, *J. Colloid Sci.*, **2**, 429 (1947). Present authors also confirmed this.

(8) T. Sasaki, unpublished.

(9) J. M. Perri and F. Hazel, *J. Phys. Colloid Chem.*, **51**, 661 (1947).

(10) W. C. Tolman, A. G. Brown and J. W. McBain, *J. Am. Chem. Soc.*, **71**, 3129 (1948).

plausible explanation. Burcik[12] and Matalon[13] explained the foam formation upon somewhat different viewpoint. Burcik emphasized the importance of the change with the time of the surface tension, and regarded the surface viscosity to be required only in the case of a remarkable foam formation. Our systems are considered to belong rather to the latter case, but a more precise explanation of the mechanism should be made in future.

Summary

1. The surface viscometer, the main part of which consisted of a fine vertical thread of glass carrying a horizontal platinum wire at its lower end, was devised for the measurement of the surface viscosity of solutions.

2. The measurements of the surface viscosity as well as some other surface properties of solutions of a number of dyes and saponin were carried out. The effect of coexisting alcohol and inorganic electrolyte for the saponin solution were also examined. The results showed a close correlation between the surface viscosity, the life of foam and so called membrane effect.

The cost of this research was defrayed from the Scientific Research Expenditure of the Department of Education.

Department of Chemistry, Faculty of Science, Kyûsyû University, Fukuoka

(11) M. Nakagaki, This Bulletin, **23**, 127 (1950).
(12) E. J Burcik, *J. Colloid Sci.*, **5**, 421 (1950).
(13) R. Matalon, *Compt. rend.*, **227**, 634 (1948).

Studies on Monomolecular Films. VI. On the Surface Films of Diphenylsiloxane Polymers

By Ryôhei MATUURA

(Received June 14, 1951)

Introduction

Recently the studies on organosiloxane polymers have become very active and extensive because of their practical importance and structural chemical interests. A great many compounds have been synthesized and their physical and chemical properties have been discussed. As to the surface chemical properties of organosiloxane polymers, the elaborate works have been performed by Hunter *et al.*,[1] Zisman *et al.*[2], and Newing[3]. They studied the surface tension, spreading and monolayer formation on the surface of water and the built-up film and the lubricating property of silicones, but the substances used in these experiments were chiefly the linear polymers. It is hoped to elucidate the surface chemical properties of the cyclic polymers as well. So it is attempted in the present work to investigate the surface films of the cyclic diphenylsiloxane trimer on water and compare their properties with those of the linear one.

Experimental

Apparatus.—The film balance used in this experiment is the same as described already.[4]

Material.—Diphenylsiloxane polymers were prepared with the method of Kipping.[5] That is, diphenyldichlorosilane (B. P. 200—210° at 45mm. Hg), prepared by the Grignard method from pure silicon tetrachloride and monobromobenzene, was hydrolysed with ice water and the resulting white solid was washed repeatedly with chloroform and petroleum ether. Then it was dissolved in the 5% potassium hydroxide solution and neutralized with acetic acid. Diphenylsilandiol thus obtained was recrystallized from acetone solution several times. For the purpose of preparing polymers of diphenylsilandiol the crystal was heated to the temperature above its melting point (132°). The polymers of various molecular structure were obtained by controlling the temperature and the period of heating, but by the suitable choice of the condition the polymers of

(1) M. J. Hunter, M. S. Gordon, A. J. Barry, J. F. Hyde and R. D. Heidenreich, *Ind. Eng. Chem.*, **39**, 1389 (1947).
(2) H. W. Fox, P. W. Taylor and W. A. Zisman, *ibid.*, **39**, 1401 (1947).
(3) M. J. Newing, *Trans. Faraday Soc.*, **46**, 755 (1950).
(4) T. Sasaki, *J. Chem. Soc. Japan*, **62**, 796 (1941); R. Matuura and I. Hayasi. *Memoris of the Faculty of Science, Kyushu University, Ser. C*, Vol. 1, 31 (1948).
(5) F. S. Kipping, *J. Chem. Soc.*, **101**, 2108, 2125 (1912); F. S. Kipping and R. Robinson, *ibid.*, **105**, 484 (1914).

rather simple and definite construction could be obtained. The film experiments were carried out with these simple polymers by spreading from benzene solution on the surface of water. The variety of samples studied are tabulated in Table 1.

Results

In Fig. 1 pressure~area curves of nine samples obtained by the procedure mentioned above are shown. The substrate is fresh distilled water (*p*H 5.4) and the temperature of experiment is 14—15°. The numeral in parentheses for the curve in Fig. 1 corresponds to

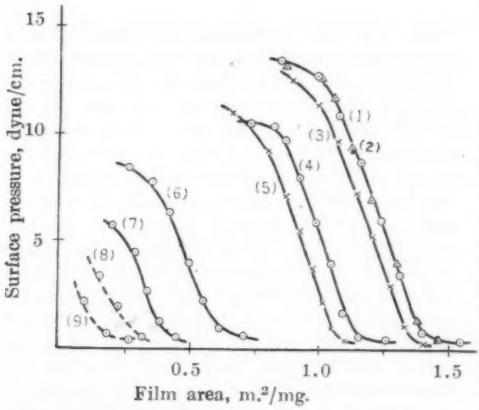

Fig. 1.—Pressure~area relations of surface films of diphenylsiloxane trimers.

that in Table 1. When the polymers of diphenylsilandiol are prepared by heating the monomer above its melting point, the dehydration takes place during the process and, therefore, the weight decreases by the amount of water lost. This decrease is shown in Table 1 as a loss of weight (in percentage). The molecular weight of each sample was determined cryoscopically in benzene solution.

Table 1

Experimental Data of Linear and Cyclic Trimers of Diphenylsilandiol and their Mixtures

No. of sample	Loss of weight, %	Molecular weight	Film area in m.²/mg.	Film area in Å.²/molec.
(1)	5.61	601	1.40	139
(2)	5.73	610	1.40	140
(3)	6.01	618	1.35	138
(4)	6.93	620	1.15	118
(5)	7.02	605	1.09	109
(6)	7.91	681	0.61	69
(7)	8.16	630	0.38	40
(8)	8.47	622	0.30	31
(9)	8.28	590	0.20	20

The samples (1) and (2) spread well and form the stable monolayers on water but the samples (3) to (7) spread with less easiness and form more and more unstable surface films as the loss of weight increases until at last in the case of samples (8) and (9) a surface film can hardly be obtained and the agglomeration readily occurs resulting in the formation of the three-dimensional crystals. The dotted lines shown in Fig. 1 represent the temporary pressure~area curves obtained by the rapid compression.

Discussion

Kipping reported several linear and two cyclic polymers obtained by the condensation of diphenylsilandiol. When diphenylsilandiol is heated above its melting point, it seems to condense first to the linear polymers and then to the cyclic ones if the chain grows long enough. The final product is, according to Kipping, mainly hexaphenylcyclotrisiloxane. In the present experiment the samples (1) and (2) consist mainly of a linear trimer and (8) and (9) of a cyclic trimer, as are confirmed by comparing the data of weight loss by the dehydration and the molecular weight observed as shown in Table 1 with those expected from the structural formulas shown in Table 2. It seems probable that a linear trimer is readily produced by heating diphenylsilandiol above its melting point for a short period and by further heating it turns to a cyclic trimer by the dehydration between hydroxyl groups at both ends of the chain. Each of the samples (3) to (7) in this experiment is considered to be a mixture of these two compounds. This is also confirmed by the result of the molecular weight determination. Since the molecular weight of the linear trimer and the cyclic one is approximately the same, about 600, the mixture of these two is expected also to have nearly the same molecular weight as above, irrespective of the composition. This is really the case as shown in Table 1. The content of the cyclic trimer in the mixture will become larger as the loss of weight in Table 1 increases.

The monolayer of the linear trimer is very stable and occupies 1.40 m.²/mg. which corresponds to 140 Å.² per molecule, while the cyclic trimer forms no stable surface films on water, readily forming large aggregates of molecules. This difference should be accounted for from the stereochemical point of view with

Table 2

Comparison of the Observed Data with the Theoretical Ones

Structural formula	Loss of weight, %		Molecular weight	
	Theor.	Obs.	Theor.	Obs.
Linear trimer 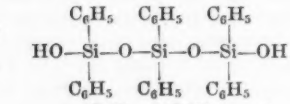	5.56	5.61 (1) 5.73 (2)	613	601 (1) 610 (2)
Cyclic trimer 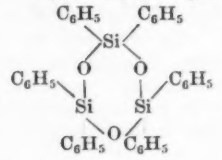	8.33	8.47 (8) 8.28 (9)	594	622 (8) 590 (9)

these two polymers. In the linear trimer, six phenyl groups can be arranged on one side of siloxane chain so that this surface is wholly nonpolar while the opposite surface, consisting of siloxane chain, is polar. That is, the molecule is clearly separated into polar part of siloxane chain and nonpolar part of phenyl groups. This polar-nonpolar character of the linear trimer is essential for it to form a stable monolayer on the surface of water. Here, of course, two hydroxyl groups attached to both ends of the chain will play a role in the film formation by anchoring to the surface of water. On the other hand, in the cyclic trimer the polar siloxane chain is almost completely concealed among six phenyl groups with no anchoring groups appearing on the surface of molecule. This leads to the lack of formation of the stable surface films on water.

The difference in the molecular structure mentioned above can also be confirmed by the experiment on the stabilization of emulsion. Namely, the benzene~water emulsion of a suitable composition was remarkably stabilized by the linear trimer but little by the cyclic trimer. This is interpreted in such a manner that the molecule of the linear trimer which has a decided polar-nonpolar structure plays an important role in stabilizing benzene~water emulsion, while that of the cyclic trimer which lacks such a structure does not. It is natural that the samples (3) to (7), being presumably the mixture of these two compounds, should be intermediate in the surface chemical properties. In fact, as mentioned already, the mixture becomes less and less spreadable as the content of the cyclic trimer increases.

Adam[6] reported that the area per phenyl group attached to the end of the hydrocarbon chain is 24 Å.^{2} Assuming this value also in the present experiment, six phenyl groups of the diphenylsiloxane trimer should occupy the area of 144 Å.^{2}, if the area of each phenyl group takes part in the area of the molecule as a whole. This is very close to the molecular area (140 Å.^{2}) of the linear trimer obtained in this experiment. Therefore it is allowed to assume that six phenyl groups are packed compactly in the film, rendering the upper film surface completely hydrophobic. This also explains the remarkably water repellent nature of the silicon film as pointed out by many workers[7]. On the other hand in the cyclic trimer, the molecular area should not be less than 72 Å.^{2}, the area of three phenyl groups, no matter how the molecule may orient itself. The reason is that, since the siloxane ring in the cyclic trimer has been confirmed to be planar[8], two phenyl groups attached to every silicon atom may overlap when projected on a horizontal plane if the molecule is oriented in such a way that the plane of the siloxane ring is horizontal, and it is impossible for the molecule to be oriented in any other way to occupy the area smaller than this. The molecular area of the cyclic trimer observed in this experiment is far smaller than this, *i. e.*, 20Å.^{2}, showing again that the molecule is not arranged in a monomolecular way, but forms large aggregates owing to its lack of polar-nonpolar balance.

Summary

The surface films of diphenylsiloxane polymers obtained by heating the monomer above its melting point were formed on the surface

(6) N. K. Adam, *Proc. Roy. Soc.*, **A 103**, 676 (1923); N. K. Adam, W. A. Berry and H. A. Turner, *ibid.*, **117**, 532 (1928).

(7) C. A. Burkhard, E. G. Rochow, H. S. Booth and J. Hartt, *Chem. Revs.*, **41**, 97 (1947).

(8) L. K. Frevel and M. J. Hunter, *J. Am. Chem. Soc.*, **67**, 2275 (1945); E. H. Aggarwal and S. H. Bauer, *J. Chem. Phys.*, **18**, 42 (1950).

of water and their properties were discussed in connection with their molecular structure. The linear trimer formed a very stable monolayer on water and its molecular area was approximately equal to the area of six phenyl groups, while the cyclic trimer formed no surface film, readily aggregating into three-dimensional crystals. This difference was explained by the difference in molecular structure; the former has a decided polar-nonpolar structure, while the latter lacks such a structure. This was also confirmed by the experiment on emulsion stabilization.

In conclusion, the author wishes to express his sincere thanks to Prof. Tunetaka Sasaki for his guidance and encouragement given to the author during this experiment.

Chemical Institute, Faculty of Science, Kyûshû University, Fukuoka

The Etched and Corroded Surfaces of Iron Single Crystal as Revealed by Means of Electron Microscopy and Diffraction

By Shigeto YAMAGUCHI

(Received June 26, 1951)

The electron microscopic observation of the etched surface of iron single crystal made it possible to assign the crystallographic axes of iron single crystal. The corrosion of iron was here investigated with an iron single crystal thus oriented. The most inactive surface plane of ferritic crystals was the (110) plane consisting of the closest packed atoms. The Fe_3O_4 crystals formed on the etched surface of iron single crystal were oriented by microscopy and diffraction. It was explained atomistically through the results obtained that the Fe_3O_4 formed on Fe substrate might protect the substrate from corrosion.

Experimental

The single crystal used in the present study was a piece of wire (diameter: 2 mm., length: 10 mm.). This specimen was etched with an etching solution (ethanol-bromine 10:1 by vol.) for 10-30 seconds. Many etching grooves running parallel to each other were recognized by the naked eye on the side face of specimen. The oxide replica of this side face was prepared by the procedures described in the previous paper[1], and it was stripped from the substrate by Mahla-Nielsen's method[2]. The electron micrograph obtained is shown in Fig. 1, in which there are octahedral crystals (size: 50-300 mμ) oriented parallel to each other. All octahedrons found in Fig. 1 are inclined by 22° regarding the (001) planes to the replica film, as is illustrated in Fig. 2. The (111) planes of these octahedrons are inclined by 32° to the replica film (*vid.* Fig. 2). The other octahedral planes $(\bar{1}11)$, $(1\bar{1}1)$ and $(\bar{1}\bar{1}1)$ planes are inclined by 56°, 56° and 70° to the replica film respectively. These inclination angles are larger than 32°. (The inclination angles given here are not strict, but within the limits of error ±5°.)

The electron beam running parallel to the etching grooves of specimen gave a diffraction pattern of Fig. 3. Fig. 3 verifies the existence of α-iron single crystal, whose (001) planes are inclined by 29° to the macroscopic surface of specimen given by shadow edge in diffraction pattern. This fact is in accordance with the results obtained in microscopy (29°≈22°). It is concluded in this way that the etched face of iron single crystal was composed of the (111) and its equivalent planes, as is shown in Fig. 2.

The electron beam running vertical to the replica film of Fig. 1 gave a diffraction pattern of Fig. 4, which verified the existence of oriented Fe_3O_4 crystals. It was comprehended through Fig. 4 that the incident beam was parallel to one of the principal axes of Fe_3O_4 crystal. When c-axis of Fe_3O_4 crystal was selected as this principal axis, the (102) plane of Fe_3O_4 was approximately parallel to the (111) plane of Fe substrate; because the angle between the (102) and the (001) planes of Fe_3O_4 was 27°, and that between the (111) planes of Fe and the replica film (*vid.* Fig. 2) was 32°, *i. e.*, 27°≈32° (*vid.* Fig. 5a). The equivalent planes of (111) shown in Fig. 2 were so steep inclined by 56° and 70° to the replica plane or macroscopic plane of specimen, that these planes were opaque for electrons (*vid.* Fig. 1). Therefore, the diffraction pattern of Fig. 4 had to be given only by the replica part of the (111) faces of Fe

(1) S. Yamaguchi, *J. Appl. Phys.*, **22**, 680 (1951).
(2) E. M. Mahla and N. A. Nielsen, *J. Appl. Phys.*, **19**, 373 (1948).

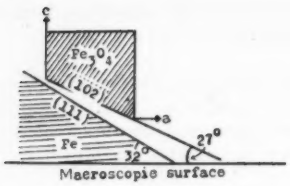

Fig. 5a.

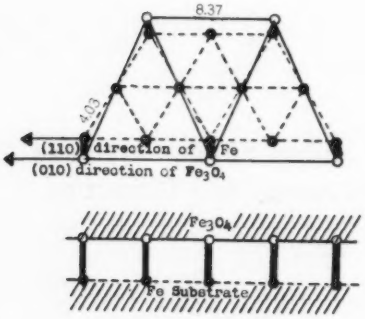

Fig. 5b.

substrate inclined by 32° to the macroscopic face of specimen. The relation between the (102) plane of Fe_3O_4 and the (111) plane of Fe substrate is shown atomistically in Fig. 5b by taking into consideration the etching grooves directed in Figs. 1, 2, 3 and 4. (The (010) direction of Fe_3O_4 was parallel to the (110) direction of Fe substrate, because the etching grooves were parallel to the (010) direction to Fe_3O_4 and to the (110) one of Fe.)

Discussion

Activity of Metal Faces.—According to the previous report of the present author[3], the corrosion rate of metal crystals depended on the activities of boundary lattice planes of crystals. So far as the cubic face-centred metal crystals were concerned, the (111) planes, which consist of the closest packed atoms, was most inert among the lattice planes. The (110) plane with coarse atom density was most active among the principal planes. In the cubic body-centred metal crystals there was a relation between the activities and the indices of lattice planes, which was quite similar to the case of cubic face-centred metal.

The (110) faces of cubic body-centred metal, whose atomic density is largest among the lattice planes, was most inert among the surface lattices of this metal. The etched surface of Fe-Cr alloy (Cr: 13 %) was composed of the dodecahedral (110) and its equivalent planes (*vid.* Fig. 6)[4], so that it was considerably corrosion-resisting. (The specimen of Fig. 6 was a rolled plate. Etchant: methanol-bromine, 100:1 by vol.) On the contrary, iron single crystal composed of the (111) and its equivalent planes, which were shown in Fig. 1, became mat more rapidly in the air at room temperature than Fe-Cr alloy of Fig. 6.

According to the theory of ionization series, Cr is by no means more inactive than Fe. Nevertheless, Fe-Cr alloy is more corrosion-resisting than pure Fe. This is due to the fact that there are the dodecahedral planes of cubic body-centred crystal on the substrate surface. The Cr in Fe-Cr alloy gives rise to the (110) planes on the etched surface of ferritic crystal.

Nature of Protective Film. — It was reported by Nelson that the $(\sqrt{2}\,\bar{1}\,0)$ direction of Fe_3O_4 formed on iron was parallel to the (111) direction of substrate[5]. The results obtained in the present study did not agree with those of Nelson.

The (102) plane of Fe_3O_4 is composed of Fe^{++} only. It is possible that these Fe^{++} ions and the Fe atoms of α-iron combine chemically with each other by exchanging their valency electrons. In cosequence of this, the Fe_3O_4 crystals can adhere solid to the metal substrate. Metal substrate is protected from further corrosion by being masked with the corrosion products, especially when the corrosion products are not only stable, but also adhere to the substrate under the given conditions. One of the Fe^{++}-Fe^{++} distances in the (102) plane of Fe_3O_4 is 8.37 Å. and the Fe-Fe distance in the (111) plane of iron is 4.03 Å. $8.37 \approx 4.03 \times 2$. It is, therefore, plausible to give a boundary structure between oxide and metal, as is shown in Fig. 5b. The experimental results on the corrosion products of metals and alloys might be referred to the previous papers of the present author[6].

Steps of Corrosion.—The corrosion of metals should be divided into the following two steps: In the first step of corrosion the rate depends on the indices of surface lattices, *i. e.*, here this is determined by the activities of the surface lattice planes. (The rate will be expressed in a form of $e^{-E/kT}$ in this case.) In the second step of corrosion the rate depends on the properties of the corrosion products

(3) S. Yamaguchi, This Bulletin, **24**, 122 (1951).

(4) The angles measured in a (110) plane in Fig. 6 coincided approximately with those of a geometrically exact dodecahedron.

(5) H. R. Nelson, *J. Chem. Phys.*, **5**, 252 (1937).

(6) S. Yamaguchi, This Bulletin, **18**, 53 (1943); S. Yamaguchi, T. Nakayama and T. Katsurai, J. Electrochem. Soc., **95**, 21 (1949).

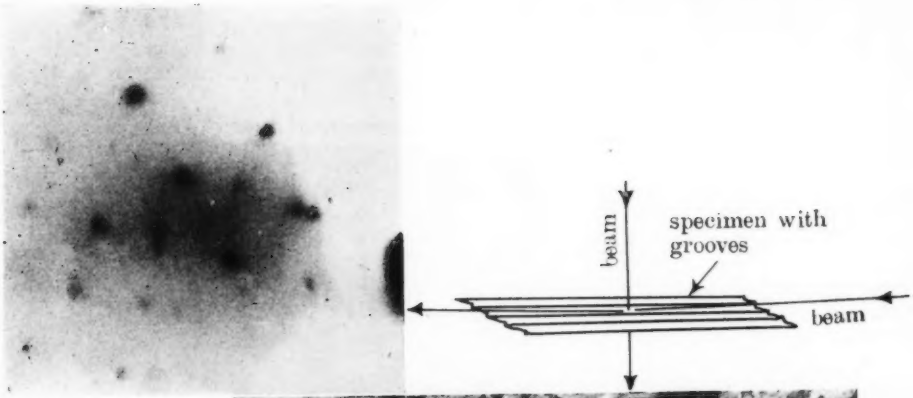

Fig. 3.

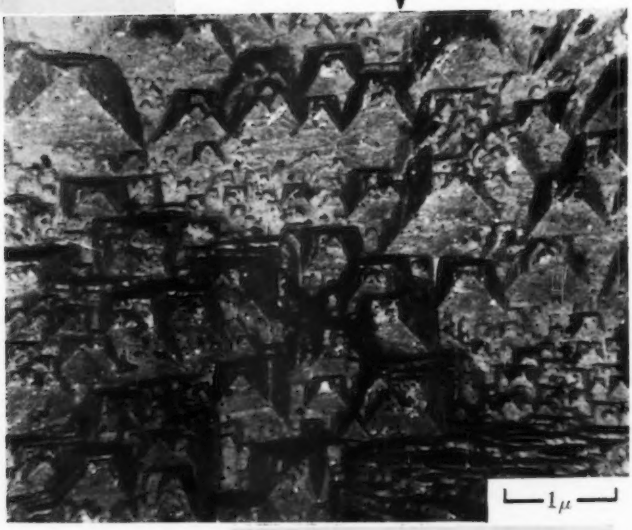

Fig. 1.

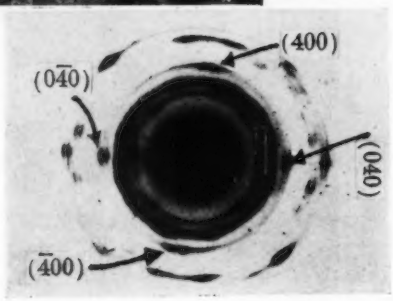

Fig. 4.

Fig. 1.—A magnified image of oxide replica formed on the etched surface of iron single crystal.

Fig. 3.—A reflection pattern obtained with the beam running parallel to the etching grooves of specimen.

Fig. 4.—A diffraction pattern obtained with the beam running perpendicular to the replica film of Fig. 1.

[*To face page 238.*

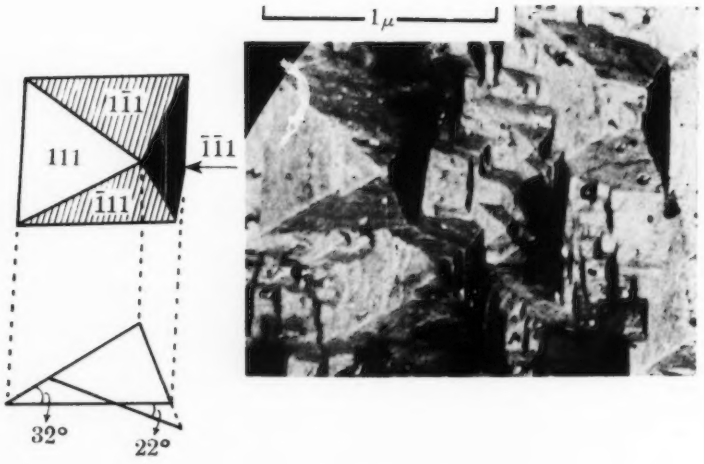

Fig. 2.—The etched surface of iron single crystal: the inclination angle between the (001) plane of octahedron and the replica film is shown schematically.

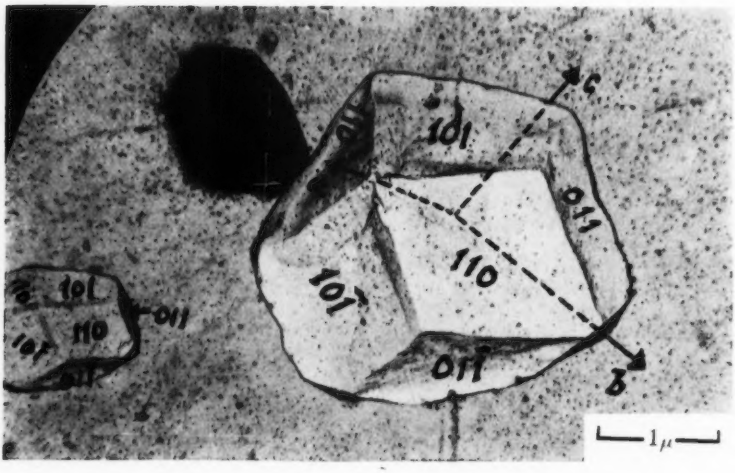

Fig. 6.—The etched surface of ferritic Fe-Cr alloy composed of the dodecahedral (110) and its equivalent planes.

formed over the metal surface. When the corrosion products on metals are exfoliated from the substrate ("erosion"), the corrosion of the first step takes place again. The dissolution of sodium in water is the typical corrosion, in which the first step is held until the end of corrosion. The formation of passive state, which is realizable on iron in nitric acid, is the typical corrosion of the second step.

Summary

1. It has been demonstrated in the present study that the single crystal of pure iron can be oriented by means of electron microscopy and diffraction in order to cut the single crystal along the desired planes. The single crystal of iron was oriented hitherto only by x-ray and optically[7].

2. The (110) faces of the cubic body-centred ferritic alloys was most inert among their surface lattices. Chromiun in 13 Cr stainless steel should be added to iron in order to give rise to the inert (110) planes on the substrate surface.

3. The etched surface of iron single crystal was composed of the (111) and its equivalent planes. The (102) planes of Fe_3O_4 crystals formed on this surface were parallel to the (111) planes of substrate. And the (010) direction of the former was parallel to the (110) direction of the latter. This fact signified that the (102) planes composed of Fe^{++} might be soldered to the (111) planes of iron by exchanging of residual valency electrons. As a matter of fact, the Fe_3O_4 film formed on iron under the given conditions serves as protective coating for substrate.

4. The corrosion of metals depends either on the activities of surface lattice planes of metals or on the properties of the corrosion products formed on surfaces.

I desire to thank Prof. N. Kameyama, Prof. I. Iitaka and Prof. S. Mizushima, who have always given the author encouragement in carring out this study.

Scientific Research Institute, Ltd.,
31 Kamifujimae Komagome, Bunkyo-ku,
Tokyo, Japan

(7) J. G. Walker, H. J. Williams and R. M. Bozorth, *Rev. Sci. Instr.*, **20**, 947 (1949).

Synthetic Studies on Thiothreonines. II

By Mitsuhiro KINOSHITA and Sumio UMEZAWA

(Received July 17, 1951)

Several investigations that have been carried out recently in our laboratory were motivated by a desire to study the method for the preparation of certain thiothreonine derivatives via threonines. In a previous paper[1], it was shown that ethyl DL-α-benzamido-β-chlorobutyrate, m. p. 84.5-86.5°, was obtained from DL-threonine, when the methyl ester of the latter was chlorinated with phosphorus pentachloride in acetyl chloride, hydrolyzed, benzoylated and finally esterified with ethanol. On the other hand, from DL-allothreonine another diastereoisomer of ethyl DL-benzamido-β-chlorobutyrate, m. p. 99-100°, was obtained by an analogous process. Recently D. F. Elliot[2] reported on the formation of these subtances from ethyl α-benzamido-β-hydroxybutyrate. The present study[3] deals with the chlorination of DL-N-benzoylallothreonine ethyl ester and the formation of thiothreonine derivatives.

Chlorination of DL-N-benzoylallothreonine ethyl ester with thionyl chloride in benzene in the presence of pyridine afforded the lower-melting isomer of ethyl DL-α-benzamido-β-chlorobutyrate in a yield of 57%, while on the contrary, chlorination with phosphorus pentachloride in chloroform afforded the higher-meltiug isomer. Thus we found[4] that

(1) M. Kinoshita and S. Umezawa, *J. Chem. Soc. Japan, Pure Chem. Sect.*, **72**, 382 (1951).

(2) D. F. Elliott, *J. Chem. Soc.*, **1949**, 589-594.

(3) The present paper was read by one of the authors (M. K.) at the 4 th Annual Meeting of the Chemical Society of Japan in Tokyo held on April 6, 1951.

one of the two diastereoisomers of ethyl DL-α-benzamido-β-chlorobutyrate was obtained depending on the experimental conditions, apparently one of these chlorinating agents causing the Walden inversion.

Replacement of the chlorine atom of the two diastereoisomers of ethyl DL-α-benzamido-β-chlorobutyrate by the sulfhydryl group could be accomplished by the action of benzyl mercaptan. We found that the reaction of the two isomers of ethyl DL-α-benzamido-β-chlorobutyrate with benzyl mercaptan in absolute ethanol in the presence of sodium ethylate gave a separable mixture of the two isomers of α-benzamido-β-benzylmercatobutyric acid. The benzene-soluble isomer melted at 136-141° and gave β-phenylethylamine salt, m. p. 166-168°, which afforded a pure free acid, melting at 145-147°, namely, N-benzoyl-S-benzylthiothreonine A. The benzene-insoluble isomer melted at 181-185° and this corresponded to the N-benzoyl-S-benzylthiothreonine B. These preparations showed no mixed melting point depression with the specimens prepared by the azlactone synthesis as reported by Carter *et al*[4]. The replacement reaction under the above conditions caused apparently some inversion. In contrast, a single racemic thiothreonine derivative was obtained when the reaction was carried out in such a non-polar or less polar solvent as benzene or ether. The reaction of benzyl mercaptan with the two isomers of ethyl α-benzamido-β-chlorobutyrate in benzene or ether led to the same N-benzoyl-S-benzylthiothreonine A as the sole product isolated. From the two isomers of α-benzamido-β-benzylmercaptobutyric acid were obtained thiothreonine A and B as Carter has described already.

Experimental

DL-N-Benzoylallothreonine Ethyl Ester.—A suspension of DL-N-benzoylallothreonine (5 g., m. p. 176°) in a solution of absolute ethyl alcohol (100 cc.) and conc. sulfuric acid (0.76 cc.) was refluxed for 3 hours. After the addition of water (0.7 cc.) solid sodium bicarbonate was added until the mixture became neutral to Congo red. The filtered solution was concentrated to a syrup under reduced pressure, and the residue was taken up in benzene. The benzene extract was concentrated again to a viscous oil. The crude ethyl ester of DL-N-benzoylallothreonine was dissolved in a small amount of dry benzene, and petroleum ether was added to this solution. The separated oil solidified after standing for several hours, yielding crude ester (5.4 g.). The recrystallization of the crude material from benzene-petroleum-ether yielded colourless needles, m. p. 84-86° (2.7 g.). Recrystallization twice from benzene raised the melting point up to 87-89.3°. By further repetition of recrystallization the melting point could not be raised further, elementary analysis showing a fair coincidence with the theoretical value (Found: N, 5.54. Calculated for $C_{13}H_{17}O_4N$: N, 5.58%). J. Attemburrow *et al.*[5] have described this substance as having a higher melting point of 98.5-101.5°.

Ethyl α-Benzamido-β-chlorobutyrate. (i) Chlorination of N-benzoyl-DL-allothreonine ethyl ester with thionyl chloride.—A solution of dry pyridine (0.49 cc.) and thionyl chloride (0.74 cc.) in dry benzene was added to a suspension of DL-N-benzoylallothreonine (1.7 g.) ethyl ester in dry benzene (11 cc.). The mixture was heated on a boiling water-bath for 20 minutes. After cooling, the mixture was washed with water, dil. hydrochloric acid, a saturated sodium bicarbonate solution in turn, and finally with water. The benzene was removed under reduced pressure. A red-brown crystalline mass (1.3 g.) was obtained. Recrystallization from petroleum ether with charcoal gave colourless plates of ethyl α-benzamido-β-chlorobutyrate, m. p. 84.5-86.5° (1 g., yield 57%); the mixed melting point with an authentic sample (cf. the previous report[1]) showed no depression.

(ii) Chlorination of DL-N-benzoylallothreonine ethyl ester with phosphorus pentachloride.—Phosphorus pentachloride (0.85 g.) was dissolved in a solution of DL-N-benzoylallothreonine ethyl ester (1 g.) in chloroform (10 cc.) cooled with ice-water. After refluxing several minutes on a water-bath, the mixture was cooled and then washed with water, dil. hydrochloric acid, a sodium bicarbonate solution in turn, and finally with water again. The chloroform was distilled off, leaving a syrup. The syrup was extracted with hot petroleum ether. When the extract was cooled, colourless prisms, m. p. 98-99°, were obtained, and recrystallization from the same solvent gave colourless prisms of ethyl α-benzamido-β-chlorobutyrate, m. p. 99-100°. The melting point was not depressed on admixture with the higher-melting specimen obtained from DL-α-benzamido-β-chlorobutyric acid (cf. the previous report[1]).

α-Benzamido-β-benzylmercaptobutyric Acids. (A) The reaction of the two isomers of ethyl α-benzamido-β-chlorobutyrate with sodium benzyl mercaptide in absolute alcohol.—(i) A solution of benzyl mercaptan (0.19 g.) in a 12% sodium ethoxide solution (0.86 cc.) was added to a solution of the higher-melting ethyl DL-α-benzamido-β-chlorobutyrate (0.4 g., m. p. 99-100°) in absolute alcohol (0.6 cc.). After heating on a water-bath for 30 minutes, the precipitated sodium chloride

(4) H. E. Carter, C. M. Stevens and L. F. Ney, *J. Biol. Chem.*, **139**, 247-254 (1941).

(5) J. Attemburrow, D. F. Elliott and G. F. Penny, *J. Chem. Soc.*, **1948**, 310-18.

was filtered off, and the alcohol was distilled under reduced pressure. The residue was taken up in ether and evaporated, leaving ethyl α-benzamido-β-benzylmercaptobutyrate as a syrup. The syrup was dissolved in a hot mixture of glacial acetic acid (3.8 cc.), conc. hydrochloric acid (1.1 cc.), and water (2.3 cc.). The solution was refluxed for 50 minutes and allowed to cool overnight. The crystalline precipitate was filtered and washed with 50% acetic acid and then with water, yielding a mixture of the two isomers of α-benzamido-β-benzylmercaptobutyric acid (230 mg., yield 47%). The mixture was extracted with two portions of boiling benzene (1.8 cc. and 1 cc.). From the residue was obtained the crude material melting at 176-183° (25 mg.). Recrystallization from benzene-alcohol gave colourless crystals, m. p. 181-185°, not depressed by mixing with the S-benzyl-N-benzoylthiothreonine B obtained by Carter's azlactone method. (Found: N, 3.95. Calculated for $C_{18}H_{19}O_3NS$: N, 4.26%). The combined benzene extract was cooled and a material melting at 136-141° was obtained (100 mg.). This material was converted into the β-phenylethylamine salt, m. p. 166-8°, by treating with β-phenylethylamine in hot ethyl acetate. By the decomposition of the salt we obtained, colourless plates, m. p. 145-7°, which were not depressed by mixing with S-benzyl-N-benzoyl thiothreonine A obtained by Carter's method (Found: N, 3.95. Calculated for $C_{18}H_{19}O_3NS$: N, 4.26%).—(ii) The lower-melting ethyl DL-α-benzamido-β-chlorobutyrate (m. p. 84-86°) was treated with benzyl mercaptan in sodium ethoxide under the same conditions as described above, giving crude S-benzyl-N-benzoyl thiothreonine A melting at 136-141° (107 mg.) and S-benzyl-N-benzoyl thiothreonine B melting at 176-183° (20 mg.).

(B) The reaction of the two isomeric ethyl α-benzamido-β-chlorobutyrates with sodium benzylmercaptide in absolute benzene. — (i) Sodium (0.02 g.) in absolute methanol (0.18 cc.) was treated with benzyl mercaptan (0.098 g.) and the solvent was removed *in vacuo*. The white sodium benzylmercaptide was covered with dry benzene, and a solution of ethyl α-benzamido-β-chlorobutyrate (0.2 g., m. p. 99-100°) in dry benzene was added. The mixture was refluxed for 2 hours on a water-bath. The mixture was filtered and the benzene was distilled under reduced pressure. The residue was extracted with ether, and ether evaporated, leaving ethyl α-benzamido-β-benzylmercaptobutyrate as a syrup. The syrup was dissolved in a hot solution of glacial acetic acid (1.87 cc.), conc. hydrochloric acid (0.57 cc.) and water (1.13 cc.). The solution was refluxed for 50 minutes and allowed to cool overnight. The crystalline precipitate was washed with 50% acetic acid and with water, yielding a crude material melting at 134-141° (110 mg., 45%). Almost all portions of this product were soluble in boiling benzene. From the benzene extract crystals melting at 136-141° were obtained (70 mg.), and the melting point was not depressed by mixing with the crude S-benzyl-N-benzoyl thiothreonine A (m. p. 136-141°) described in (A). (ii) The lower-melting ethyl DL-α-benzamido-β-chlorobutyrate (0.2 g., m. p. 84-6°) was treated with sodium benzylmercaptide in dry benzene under the same conditions, and hydrolyzed as described above, giving a crude product melting at 130-136° (65 mg.). S-benzyl-N-benzoyl thiothreonine A melting at 136-141° (41 mg.) was obtained from the benzene-soluble part.

(C) The reaction of ethyl α-benzamido-β-chlorobutyrate with sodium benzylmercaptide in absolute ether. — Sodium benzylmercaptide, which was prepared by the same method as described in (B), was covered with dry ether and an etherial solution of lower-melting ethyl DL-α-benzamido-β-chlorobutyrate (0.2 g., m. p. 84-86°) was added. The mixture was refluxed in a water-bath at 60° for 15 minutes, and the subsequent treatment was accomplished as mentioned above. A crude product (112 mg.) melting at 128-138° was obtained. From benzene extract, S-benzyl-N-benzoyl thiothreonine A (75 mg.) melting at 136-141° was obtained.

Summary

(1) Chlorination of DL-N-benzoylallothreonine ethyl ester with thionyl chloride in benzene in the presence of pyridine gave the lower-melting isomer of ethyl DL-α-benzamido-β-chlorobutyrate, m. p. 84.5-86.5°, in a yield of 57%. On the other hand, chlorination with phosphorus pentachloride in chloroform gave the higher-melting isomer, m. p. 99-100°.

(2) Two isomers of α-benzamido-β-benzylmercaptobutyric acid (derivatives of thiothreonine A and B) were synthesised. The chlorine atom of ethyl DL-α-benzamido-β-chlorobutyrate could be replaced by a sulfhydryl group by the action of benzyl mercaptan. A remarkable effect of different solvents on this replacement reaction was described.

A part of the cost of the present research has been defrayed from the Scientific Research Encouragement Grant from the Ministry of Education, to which the authors' thanks are due.

Department of Applied Chemistry,
Engineering Faculty of Keio University, Tokyo

Calculation of the Diamagnetic Anisotropy of Benzene by the Method of Antisymmetric Molecular Orbitals

By Saburo FUJII and Shoji SHIDA

(Received July 20, 1951)

Introduction

Cyclic molecules[1] composed of conjugated double bonds, such as aromatic compounds,[2] have a remarkable degree of diamagnetic anisotropy in the directions perpendicular to the molecular planes. For instance, the observed value of the anisotropy for benzene is about -54×10^{-6} ergs per gauss per mole[3]. This phenomenon is generally recognized to be caused by the free migration of the resonating $p\pi$-electrons along the molecular network under an external magnetic field. The quantum mechanical theories of the effect in aromatic molecules have been worked out by F. London[4] and by H. Brooks,[5]·[6] who calculated the ratio of the anisotropies of the various condensed ring compounds to that of benzene. In London's theory[4] based on the simple method of molecular orbitals the calculated results are in good agreement with experiments, but his theory neglects the Pauli's exclusion principle and also the correlation effects between electrons. On the other hand H. Brooks[6] treated anisotropy from the standpoint of the Heitler-London-Pauling-Slater approximation including ionic structures and amended the weakness of London's method, but his results are not better than London's in spite of his great labor. Furthermore both theories can not calculate the absolute value of the anisotropy for benzene.

The present paper is an effort to treat the diamagnetic anisotropy of benzene from the standpoint of the method of antisymmetric molecular orbitals (Goeppert-Mayer and Sklar's metod[7]) and to calculate the absolute value of the anisotropy. The G-M-S method has given a satisfactory result in the calculation of the lower excited levels of benzene and therefore it is interesting to see what results we can get from this method for the present purpose.

The Orbitals

When the magnetic field $\mathbf{H}$ is applied in the direction perpendicular to the plane of benzene molecule, the orbital of the ν-th π-electron in the l-th energy level may be described according to London's method:

$$\left.\begin{aligned}\phi_l&=(6\sigma_l)^{-\frac{1}{2}}\sum_{k=1}^{6}e^{\frac{2\pi l}{6}kl+f)}\times e^{i[\vec{\alpha}(k)\cdot\vec{r}_\nu]}\times U_k(\nu),\\ l&=0,\pm1,\pm2,3,\quad \phi_l^*\equiv\phi_{-l}\text{[8]},\end{aligned}\right\}\quad(1)$$

where $U_k(\nu)$ is the $2p\pi$ wave function of the k-th carbon atom at $\mathbf{H}=0$ and σ_l the normalization factor ($\sigma_l=1$ in London's paper). Also $\vec{\alpha}(k)=\frac{2\pi e}{hc}\vec{\mathbf{A}}(r_\epsilon)$, $\vec{\mathbf{A}}(r_k)$ [9] being the vector potential in the position of the k-th nucleus; $f=\frac{e}{hc}S\cdot\mathbf{H}$, S being the area of the benzene ring. Here the orbitals ϕ_l are mutually orthogonal and $U_k(\nu)$ assumed to be normalized.

If the treatment for the vector potential is similar to that in London's paper, the normalization factors σ_l are then determined by the relation:

$$\sigma_l=1+2S_1\cos\frac{2\pi}{6}(l+f)+2S_2\cdot\cos\frac{2\pi}{6}(2l+f)+(-1)^l\cdot S_3,\quad(2)$$

where

$$S_l=\int U_1(\nu)\cdot U_{1+l}(\nu)d\tau_\nu$$

(overlap integrals at $\mathbf{H}=0$).

The energy of the molecule is the lowest if the

(1) Cycloöctatetraene C_8H_8 is excepted: see S. Shida and S. Fujii, This Bulletin, **24**, 173 (1951).

(2) K. Lonsdale, *Reports on Progress in Physics*, **4**, 368 (1937).

(3) K. Lonsdale and K. S. Krishnan, *Proc. Roy. Soc. London*, **156 A**, 597 (1937).

(4) F. London, *J. phys.*, **8**, 397 (1937).

(5) H. Brooks, *J. Chem. Phys.*, **9**, 463 (1941).

(6) H. Brooks, *J. Chem. Phys.*, **8**, 939 (1940).

(7) M. Goeppert-Mayer and A. L. Sklar, *J. Chem. Phys.*, **6**, 645 (1938).

(8) ϕ_l^* is the complex conjugate of ϕ_l. $\phi_l^*=\phi_{-l}$ for $\mathbf{H}=0$.

(9) If the direction perpendicular to the molecular plane is chosen to be Z-axis,

$$\vec{\mathbf{A}}=(A_x,A_y,A_z)=\left(-\frac{1}{2}y\mathbf{H},\frac{1}{2}x\mathbf{H},0\right).$$

orbitals $\phi_0, \phi_1, \phi_{-1}$ contain two electrons each; the perturbation energy caused by the magnetic field is usually very small. Therefore it is not necessary, for the present purpose, to consider the excited levels $l=\pm 2, 3$. Then the eigenfunction of the lowest state in this order of approximation is represented by

$$\Psi_0=\phi_0(1)\phi_0(2)\phi_1(3)\phi_1(4)\phi_{-1}(5)\phi_{-1}(6).$$

Also the total spin function in this state is the product

$$\chi_0=\alpha(1)\beta(2)\alpha(3)\beta(4)\alpha(5)\beta(6),$$

for the lowest state is experimentally diamagnetic.

The totally antisymmetric eigenfunction for this state is then obtained as follows,

$$\Psi_0=(6!)^{-1/2}\sum_p(-1)^p\mathbf{P}(\psi_0\chi_0), \qquad (3)$$

where $\mathbf{P}$ is the permutation operator.

The Calculation of Energy in a Magnetic Field

The Hamiltonian for the benzene molecule in the magnetic field may be written[4),(7)]:

$$\mathcal{H}=\sum_\nu\left\{\frac{h^2}{8\pi^2 m}\left(\frac{1}{i}\vec{\nabla}_\nu+\vec{\alpha}_\nu\right)^2+\sum_k V_{\nu k}\right\}+\sum_{\substack{\nu=1\\ \mu<\nu}}^{6}\frac{e^2}{r_{\nu\mu}}, \qquad (4)$$

where $\vec{\alpha}_\nu=\frac{2\pi e}{hc}\vec{\mathbf{A}}_\nu$, $\vec{\mathbf{A}}_\nu$ being the vector potential which acts in the ν-th electron. $V_{\nu k}$ is the potential of the k-th carbon nucleus acting on the ν-th lelctron and may be represented as follows,

$$V_{\nu k}=\mathbf{H}_{\nu k}-\int\frac{e^2}{r_{\nu\mu}}U_k^2(\mu), \qquad (5)$$

where $\mathbf{H}_{\nu k}$ is the potential of the neutral carbon atom. The average value of the Hamiltonian $\mathcal{H}$ in this state is given by

$$E=\int\int\cdots\int\Psi_0^*\mathcal{H}\Psi_0\,d\tau_1 d\tau_2\cdots d\tau_6. \qquad (6)$$

If we put

$$\left.\begin{aligned}\varepsilon_l&=\int\phi_l^*(\nu)\left\{\frac{h^2}{8\pi^2 m}\left(\frac{1}{i}\vec{\nabla}_\nu+\vec{\alpha}_\nu\right)^2+\sum V_{\nu k}\right\}\phi_l(\nu)d\tau_\nu,\\ \gamma_{ll'}&=\int\frac{e^2}{r_{\nu\mu}}[\phi_l(\nu)\phi_l^*(\nu)][\phi_{l'}(\mu)\phi_{l'}^*(\mu)]d\tau_\nu d\tau_\mu,\\ \delta_{ll'}&=\int\frac{e^2}{r_{\nu\mu}}[\phi_l(\nu)\phi_{l'}^*(\nu)][\phi_{l'}(\mu)\phi_l^*(\mu)]d\tau_\nu d\tau_\mu,\end{aligned}\right\} \qquad (7)$$

then the total energy in the magnetic field $\mathbf{H}$ is

$$\begin{aligned}E&=(2\varepsilon_0+2\varepsilon_1+2\varepsilon_{-1})\\&\quad+\int\int\cdots\int\Psi_0^*\left(\sum_{\substack{\nu=1\\ \mu<\nu}}^{6}\frac{e^2}{r_{\nu\mu}}\right)\Psi_0 d\tau_1 d\tau_2\cdots d\tau_6\\&=(2\varepsilon_0+2\varepsilon_1+2\varepsilon_{-1})+(\gamma_{00}+4\gamma_{01}+4\gamma_{0-1}\\&\quad+4\gamma_{1-1}+\gamma_{11}+\gamma_{-1-1}-2\delta_{01}-2\delta_{0-1}-2\delta_{1-1}).\end{aligned} \qquad (8)$$

In the expansion of the integrals ε, γ, δ in terms of $\mathbf{H}$ and integrals over the atomic eigenfunctions U_k, we must treat the integrals of the form

$$\int\int e^{i[\overrightarrow{\alpha(k)}-\overrightarrow{\alpha(l)}\cdot\vec{r}_\nu]}U_k(\nu)\,U_l(\nu)\frac{e^2}{r_{\nu\mu}}\,e^{i[\overrightarrow{\alpha(m)}-\overrightarrow{\alpha(n)}\cdot\vec{r}_\mu]}\times U_m(\mu)U_n(\mu)d\tau_\nu\,d\tau_\mu. \qquad (9)$$

The rigorous calculations of these integrals are complicated. Therefore, for the first approximation, $\vec{r}_\nu$ is replaced by $\frac{1}{2}(\vec{R}_k+\vec{R}_l)$ where the product $U_k(\nu)U_l(\nu)$ has the maximum value, and $\vec{r}_\mu$ by $\frac{1}{2}(\vec{R}_m+\vec{R}_n)$ in the similar manner. Here $\vec{R}_k$, $\vec{R}_l$, $\vec{R}_m$ and $\vec{R}_n$ represent the position vectors of the correspondingly numbered nuclei. This approximation[10] may be adequate, because $e^{i[\overrightarrow{\alpha(k)}-\overrightarrow{\alpha(l)}\cdot\vec{r}_\nu]}$, $e^{i[\overrightarrow{\alpha(m)}-\overrightarrow{\alpha(n)}\cdot\vec{r}_\mu]}$ do not make large changes in the ranges of $\vec{R}_k\sim\vec{R}_l$ and $\vec{R}_m\sim\vec{R}_n$ respectively. Using this approximation, we then obtain

$$\begin{aligned}\gamma_{ll'}&=\frac{1}{6\sigma_l\cdot\sigma_{l'}}\Big[(A_0+2A_1+2A_2+A_3)\\&+2(B_1+B_2+B_3)\left\{\cos\frac{2\pi}{6}(l+f)+\cos\frac{2\pi}{6}(l'+f)\right\}\\&+2(C_1+2C_2+2C_3+C_4)\left\{\cos\frac{2\pi}{6}(l+l'+2f)+\cos\frac{2\pi}{6}(l-l')\right\}\\&+2(F_1+2F_2+2F_3+F_4)\left\{\cos\frac{2\pi}{6}(2l+f)+\cos\frac{2\pi}{6}(2l'+f)\right\}\end{aligned}$$

(10) This approximation is analogous to the one used by F. London in the calculation of the resonance integral of π-electron in a magnetic field.

$$+4(J_1+J_2+J_3)\left\{\cos\frac{2\pi}{6}(2l+l'+2f)+\cos\frac{2\pi}{6}(l+2l'+2f)+\cos\frac{2\pi}{6}(2l-l')+\cos\frac{2\pi}{6}(2l'-l)\right\}+6\{(-1)^l+(-1)^{l'}\}\cdot D\Big], \quad (10)$$

$$\delta_{ll'}=\frac{1}{6\sigma_l\cdot\sigma_{l'}}\Big[\Big\{A_0+2A_1\cos\frac{2\pi}{6}(l-l')+2A_2\cos\frac{4\pi}{6}(l-l')+(-1)^{l-l'}A_3\Big\}+4B_1\Big\{\cos\frac{2\pi}{6}(l+f)+\cos\frac{2\pi}{6}(l'+f)\Big\}+4B_2\Big\{\cos\frac{2\pi}{6}(2l-l'+f)+\cos\frac{2\pi}{6}(2l'-l+f)\Big\}+4B_3\Big\{(-1)^{l-l'}\cos\frac{2\pi}{6}(l+f)+(-1)^{l'-l}\cos\frac{2\pi}{6}(l'+f)\Big\}+2\Big\{C_1+2C_2\cos\frac{2\pi}{6}(l-l')+2C_3\cos\frac{4\pi}{6}(l-l')+(-1)^{l-l'}\cdot C_4\Big\}\Big\{1+\cos\frac{2\pi}{6}(l+l'+2f)\Big\}+4\{F_1+(-1)^{l-l'}F_4\}\cos\frac{2\pi}{6}(l+l'+f)+4\{F_2+(-1)^{l-l'}\cdot F_3\}\Big\{\cos\frac{2\pi}{6}(2l+f)+\cos\frac{2\pi}{6}(2l'+f)\Big\}+4\{J_1+(-1)^{l-l'}\cdot J_3\}\Big\{\cos\frac{2\pi}{6}(2l'+l+2f)+\cos\frac{2\pi}{6}(2l+l'+2f)+\cos\frac{2\pi}{6}l+\cos\frac{2\pi}{6}l'\Big\}+4J_2\Big\{(-1)^l\cos\frac{4\pi}{6}f+(-1)^{l'}\cos\frac{4\pi}{6}f+\cos\frac{2\pi}{6}(2l-l')+\cos\frac{2\pi}{6}(2l'-l)\Big\}+D\cdot\{(-1)^l+(-1)^{l'}\}\cdot\Big\{1+2\cos\frac{2\pi}{6}(l-l')+2\cos\frac{4\pi}{6}(l-l')+(-1)^{l-l'}\Big\}\Big], \quad (11)$$

where

$$A_l=\iint U_1^2(\nu)\frac{e^2}{r_{\nu\lambda}}U^2{}_{1+l}(\mu)d\tau_\nu\,d\tau_\mu,$$
$$B_l=\iint U_1(\nu)U_6(\nu)\frac{e^2}{r_{\nu\mu}}U_l^2(\mu)d\tau_\nu\,d\tau_\mu,$$
$$C_l=\iint U_1(\nu)U_2(\nu)\frac{e^2}{r_{\nu\mu}}U_l(\mu)U_{1+l}(\mu)\,d\tau_\nu\,d\tau_\mu,$$
$$D^{(11)}=\iint U_1(\nu)U_4(\nu)\frac{e^2}{r_{\nu\lambda}}U_l^2(\mu)d\tau_\nu\,d\tau_\mu,$$
$$F_l=\iint U_1(\nu)U_3(\nu)\frac{e^2}{r_{\nu\mu}}U^2{}_{1+l}(\mu)d\tau_\nu\,d\tau_\mu,$$
$$J_l=\iint U_1(\nu)U_2(\nu)\frac{e^2}{r_{\nu\mu}}U_l(\mu)U_{2+l}(\mu)d\tau_\nu\,d\tau_\mu. \quad (12)$$

Also, since $e^{i[\vec{\alpha}(k)\cdot\vec{r}]}U_k(\nu)$ is taken to be an atomic eigenfunction in the magnetic field **H**, the relation

$$\left\{\frac{h^2}{8\pi^2m}\left(\frac{1}{i}\vec{\nabla}_\nu+\vec{\alpha}_\nu\right)^2+V_{\nu k}\right\}e^{i[\vec{\alpha}(k)\cdot\vec{r}_\nu]}U_k(\nu)=W_{2p'}e^{i[\vec{\alpha}(k)\cdot\vec{r}_\nu]}U_k(\nu) \quad (13)$$

holds, where $W_{2p'}$ is the energy of a $2p$ electron which is in the valence state and in the magnetic field **H**. Hence ε_l, the energy of the orbital in (1), is expanded in the form

$$\varepsilon_l=W'_{2p}-\frac{2}{\sigma_l}\Big[\Big(Q+A_1+A_2+\frac{1}{2}A_3\Big)+(R_1+2R'_1+B_1+2B_2+2B_3)\cos\frac{2\pi}{6}(l+f)+(R_2+R'_2+F_1+F_2+2F_3+F_4)\cos\frac{2\pi}{6}(2l+f)+(-1)^l\cdot\Big(2R'_3+\frac{5}{2}D\Big)\Big], \quad (14)$$

where

$$Q=-\int\mathbf{H}_\nu U^2{}_2(\nu)d\tau_\nu,$$
$$R_l=-\int\mathbf{H}_\nu U_1(\nu)U_{1+l}(\nu)d\tau_\nu,$$
$$R'_l=-\int\mathbf{H}_\nu U_2(\nu)U_{2+l}(\nu)d\tau_\nu. \quad (15)$$

The functions U_k used for the numerical calculation of the integrals are $2p\pi$ hydrogen-like functions

$$U(r,\theta,\varphi)=\sqrt{\frac{Z^5}{32\pi}}\cdot r\cdot\sin\theta\cdot\cos\varphi\cdot e^{-\frac{Zr}{2}},$$

where the effective nuclear charge Z is chosen to be 3.18[12] as usual. The distance between neighboring carbon atoms is 1.39 Å. The numerical values of $A_l, B_l, C_l, D_l, F_l, J_l, R_l, R_l'$, and S_l are collected in Table 1. These adopted

(11) Here D represents D_l, but the values of D_l for all of l are the same.

(12) C. Zener, *Phys. Rev.*, **36**, 51 (1930).

data are selected by U. Mori[13], who has recalculated the numerical values of the above integrals from Parr-Crawford's[14] and Kotani-Amemiya-Simose's[15] tables and with A. London's approximation method[16].

Table 1

A_0= 16.9301 e.V.	D =0.1622 e.V.
A_1= 9.0232 e.V.	J_1 =0.1354 e.V.
A_2= 5.6669 e.V.	J_2 =0.0911 e.V.
A_3= 4.9744 e.V.	J_3 =0.0725 e.V.
B_1= 3.3184 e.V.	Q =0.8542 e.V.
B_2= 1.8681 e.V.	R_1 =1.8880 e.V.
B_3= 1.4227 e.V.	R_2 =0.1080 e.V.
C_1= 0.9516 e.V.	R_1' =0.0387 e.V.
C_2= 0.6769 e.V.	R_2' =0.0318 e.V.
C_3= 0.4357 e.V.	R_3' =0.0316 e.V.
C_4= 0.3831 e.V.	
F_1= 0.5208 e.V.	S_1 =0.2600
F_2= 0.3888 e.V.	S_2 =0.0388
F_3= 0.2790 e.V.	S_3 =0.0179
F_4= 0.2503 e.V.	

The Calculation of Anisotropy

When the magnetic field **H** is applied in the direction parallel to the molecular plane, neither $\gamma_{ll'}$ nor $\delta_{ll'}$ depends on **H**, and in the expansion of ε_l only the term W_{2p}' remains unchanged as the function of **H**, since $f=0$ in this case. Therefore the anisotropy in the direction perpendicular to the molecular plane may be written:

$$\begin{aligned}\Delta\chi_\perp &= -\left[\frac{\partial^2}{\partial H^2}(E-E^0)\right]_{H\to 0} \\ &= -\left[\frac{\partial^2}{\partial H^2}(2\varepsilon_0+2\varepsilon_1+2\varepsilon_{-1}-6W'_{2p})\right]_{H\to 0} \\ &\quad -\left[\frac{\partial^2}{\partial H^2}\left(\int\int\cdots\int\psi_0^*\left(\sum_{\substack{\nu=1\\ \mu<\nu}}^{6}\frac{e^2}{r_{\nu\mu}}\right)\right.\right. \\ &\quad \left.\left.\times\psi_0 d\tau_1 d\tau_2\ldots d\tau_6\right)\right]_{H\to 0}, \quad (16)\end{aligned}$$

where E^0 is E in the case of which **H** is

Table 2

	A	B	C
$-\left[\frac{\partial^2}{\partial H^2}(\varepsilon_0-W'_{2p})\right]_{H\to 0}$	$+4.157\left(\frac{2\pi eS}{6hc}\right)^2$,	$-2.092\left(\frac{2\pi eS}{6hc}\right)^2$,	$-2.456\left(\frac{2\pi eS}{6hc}\right)^2$,
$-\left[\frac{\partial^2}{\partial H^2}(\varepsilon_{\pm 1}-W'_{2p})\right]_{H\to 0}$	+8.221 〃	−5.160 〃	−5.712 〃
$-\left[\frac{\partial^2\tau_{00}}{\partial H^2}\right]_{H\to 0}$	−1.675 〃	+0.034 〃	+0.034 〃
$-\left[\frac{\partial^2\tau_{0\pm 1}}{\partial H^2}\right]_{H\to 0}$	−2.664 〃	+0.041 〃	+0.041 〃
$-\left[\frac{\partial^2\tau_{1-1}}{\partial H^2}\right]_{H\to 0}$	−3.158 〃	+0.110 〃	+0.110 〃
$-\left[\frac{\partial^2\tau_{11}}{\partial H^2}\right]_{H\to 0}=-\left[\frac{\partial^2\tau_{-1-1}}{\partial H^2}\right]_{H\to 0}$	−7.231 〃	−0.512 〃	−0.512 〃
$-\left[\frac{\partial^2\delta_{0\pm 1}}{\partial H^2}\right]_{H\to 0}$	+0.109 〃	−0.225 〃	−0.225 〃
$-\left[\frac{\partial^2\delta_{1-1}}{\partial H^2}\right]_{H\to 0}$	+0.665 〃	−0.319 〃	−0.319 〃
$-\left[\frac{\partial^2}{\partial H^2}(2\varepsilon_0+2\varepsilon_1+2\varepsilon_{-1}-6W'_{2p})\right]_{H\to 0}$	+41.198 〃	−24.824 〃	−27.760 〃
$-\left[\frac{\partial^2}{\partial H^2}\left(\int\int\cdots\int\psi_0^*\left(\sum_{\substack{\nu=1\\ \mu<\nu}}^{6}\frac{e^2}{r_{\nu\mu}}\right)\psi_0 d\tau_1 d\tau_2\ldots d\tau_6\right)\right]_{H\to 0}$	−51.853 〃	+ 1.840 〃	+ 1.840 〃
$-\left[\frac{\partial^2}{\partial H^2}(E-E^0)\right]_{H\to 0}$	−10.65 〃	−22.98 〃	−26.00 〃
Calculated anisotropy. (ergs per gauss per mole)	-16.2×10^{-6}	-35.1×10^{-6}	-40.0×10^{-6}
$\frac{\text{Calculated value}}{\text{Experimental value}}\times 100$, %	30	65	74

(13) One of the members in our laboratory.
(14) R. G. Parr and B. L. Crawford, *J. Chem. Phys.*, **16**, 1049 (1948); C. C. J. Roothaan and R. G. Parr, *J. Chem. Phys.*, **17**, 1001 (1949).
(15) M. Kotani, A. Amemiya and T. Shimose, *Proc. Phys.-Math. Soc. Japan*, **20**, extra number I (1938); **22**, extra number I (1940).
(16) A. London, *J. Chem. Phys.*, **13**, 396 (1945).

applied in the direction parallel to the molecular plane. The results of numerical calculations are given in Table 2. Column A in Table 2 represents the result obtained when only the types of integrals used in Goeppert-Mayer and Sklar's paper[7] are adopted. Column B is the result when all the remaining types of integrals except R_2, R'_1, R'_2, and R'_3 in Table 1 are used. Column C is derived by the use of all the integrals in Table 1.

Considerations

The best result obtained in this manner is -40×10^{-6} ergs per gauss per mole, it being about 74 percent of the experimental value -54×10^{-6}. The physical contradiction appears in the case of column A, where the contribution of ε_l to the anisotropy is paramagnetic and that of repulsions between electrons diamagnetic, in spite of the fact that the former and the latter must be physically diamagnetic and paramagnetic respectively. But this contradiction is removed in columns B and C by the use of the integrals neglected in column A, and the numerical results become better. It is natural that the calculated result approaches more and more to the experimental value as the approximation used becomes of higher order. If the approximate methods used in this paper are not unreasonable, the above considerations may be useful in the criticism of the ground states calculated by the G-M-S method and it may be concluded that the energy level $^1A_{1g}$ in their original paper is unsuitable. On the other hand we have been also taught the fact that the anisotropy is largely enhanced by the orbital effects and slightly diminished by the correlation effects between π-electrons. Thus, the reason why good results were obtained by F. London's method neglecting the correlation effects between π-electrons may be understood to some extent.

Recently the conception of configurational interaction has been introduced by Craig[17] into the antisymmetric molecular orbital treatment of the absorption spectra of benzene. According to his paper there are four A_{1g} states including the ground state (at $\mathbf{H}=0$) described in the present paper, and the interactions among this set of A_{1g} states depress the lowest of them by about 2 e.V. Therefore it is interesting and may be valuable to note that the problems of anisotropy are treated with the introduction of configurational interaction.

Summary

The absolute value of the diamagnetic anisotropy of benzene was calculated by the method of antisymmetric molecular orbitals. The value obtained was about -40×10^{-6} ergs per gauss per mole, it being about 74 percent of the experimental value.

It was found that the anisotropy was largely enhanced by orbital effects and slightly diminished by correlation effects between π-electrons.

The authors wish to express their thanks to Mr. U. Mori for his co-operation in the discussion of the atomic integrals. They also thank the Department of Education for the Scientific Research Encouragement Grant.

Laboratory of Physical Chemistry, Tokyo Institute of Technology (Tokyo Kōgyo Daigaku), Tokyo.

(17) D. P. Craig, *Proc. Roy. Soc. London*, **200 A**, 747 (1950).

On the Mechanism of Evaporation in Vacuum. II. Vapor Pressure and Evaporation Velocity.[1]

By Masayuki NAKAGAKI

(Received July 31, 1951)

It is suggested in the preceding paper[2] that the estimation of vapor pressure is valuable when discussig the evaporation of various substances. The phase diagram of one component system is composed, in the simplest case, of three curves, that is sublimation, evaporation and fusion curves. These curves are described by Clapeyron-Clausius' equation:

$$\mathrm{d}\ln p/\mathrm{d}T = L/RT^2 \qquad (1)$$

where p is pressure, T is absolute temperature, L is the latent heat of the phase transition, and R is the gas constant. This is integrated after expanding the latent heat L in power series, according to Nernst, and obtained,

$$\log p(\mathrm{mm.}) = 2.88 - L_0/4.59\,T + 1.75\log T - \varepsilon T/4.59 + \kappa \qquad (2)$$

where p (mm.) is the pressure expressed in mm. Hg., ε is a parameter determined from some experimental data, and κ is the conventional chemical constant. The latter is calculated for monoatomic gases by the following equation:

$$\kappa = -1.587 + 1.5\log M \qquad (3)$$

where M is the molecular weight. All three curves in the phase diagram cross at one point, named a triple point. At this point, in general, the heat of sublimation and the heat of evaporation are not equal, while the reationship:

$$L_{sub.} = L_{fus.} + L_{evap.} \qquad (4)$$

is obtained thermodynamically[3]. As for many metals, it is seen that,

$$L_{fus.}/L_{sub.} \simeq 0.015 \sim 0.058 \qquad (5)$$

The following approximation is, therefore, used:

$$L_{sub.} \simeq L_{evap.} \qquad (6)$$

Under this approximation sublimation and evaporation curves are described by one curve. Moreover, the melting point curve is often approximated by a straight line parallel to the pressure axis. Then, a simplified phase diagram is drawn for every metal, using the data tabulated in Table 1. For various metals, atomic weight M, and boiling point T_b inserted in the "Rika-Nenpyo"[4], and the heat of sublimation at absolute zero temperature L_0 by Slater[5] are cited in the Table. Among the data of L_0, those marked with * are values at room temperature by Seitz[6]. The difference of the latent heat at absolute zero and room temperature is, in general, negligible, since it is less than 1 kcal./mole for these metals. The value of conventional chemical constant obtained from equation (3) is cited in the fifth column. The parameter ε is calculated by equation (2), using the fact that the temperature corresponding to the pressure $p=760$ mm. Hg is the boiling point T_b; and cited on the sixth column. Then, the vapor pressure curve is drawn, using Eq. (2) and values L_0, ε, and κ, cited above. By the assumption that the temperature for the triple point is nearly equal to the melting point T_m, given in "Rika-Nenpyo"[4] and Slater's book[5], the pressure for the triple point p_t, is obtained. These are cited in the seventh and eighth column. Phase diagrams are depicted in Fig. 1 for various metals. They approximately coincide with curves by Law[7], excepting Be, Al, Cr and Fe. The disagreements will be studied later.

Yarwood[8] recorded the temperature of vacuum evaporation T_e. These values are cited in the tenth column of Table 1. The pressure in the vessel was 10^{-5} mm. Hg. The plots of these temperature data on the vapor

(1) These results were presented befor the Meeting of Colloid Chemistry held by the Chemical Society of Japan at Osaka, November, 1950.

(2) M. Nakagaki, This Bulletin, **24**, 206 (1951).

(3) J. C. Slater, "Introduction to Chemical Physics", New York, 1939, p. 172.

(4) Edited by the Tokyo Astronomical Observatory, "Rika-Nenpyo", 1950, Tokyo.

(5) J. C. Slater, *loc. cit*, pp. 259 and 454.

(6) F. Seitz, "The Modern Theory of Solid", New York, 1940, p. 3 and 61.

(7) R. R. Law, *Rev. Sci. Instr.*, **19**, 920 (1948).

(8) J. Yarwood, "High Vacuum Technique," London, 1948, pp. 84~90.

Table 1

Substances	Atomic or molecular wt. M	Boiling point T_b, °C.	Latent heat L_0 (kcal./mole)	Parameters in Eq. (2) κ	Parameters in Eq. (2) ε, cal./deg.^{2}	Triple point T_m, °C.	Triple point $\log p_t$, mm. Hg	Vacuum evaporation temp. T_e, °C. Calcd.	Vacuum evaporation temp. T_e, °C. Obsd.
Cs	132.91	670	18.7	1.599	0.0121	28.5	−7.26	200	433
Rb	85.48	700	20.6	1.311	0.0091	38.	−8.06	250	450
Cd	112.41	764	27.0	1.487	0.00487	320.9	−1.78	400	541
Zn	65.38	907	31.4	1.136	0.00288	419.5	−1.69	500	623
Mg	24.32	1110	36.6	0.491	0.00070	651.	−0.48	650	712
Li	6.94	1340	36.0	−0.325	0.00120	186.	−10.70	700	821
Sr	87.63	1150	47.0*	1.327	−0.00113	800.	0.02	700	811
Ca	40.08	1170	47.8*	0.818	−0.00280	810.	−0.15	750	878
Bi	209.00	1450	47.8	1.893	0.00405	271.	−11.00	750	913
Pb	207.21	1620	46.7	1.887	0.00547	327.3	−8.50	800	1000
Sb	121.76	1380	54.4	1.543	0.00000	630.5	−3.79	850	973
Be	9.02	(1500)	75.0*	−0.154	−0.0095	1350.	1.6	1150	—
Al	39.94	1800	67.6	0.815	−0.0011	659.	−6.7	1150	1461
Ag	107.88	1950	69.4	1.463	0.00107	960.5	−2.98	1200	1319
Sn	118.70	2260	68.0	1.526	0.00296	231.9	−21.09	1250	1148
Cu	63.54	2360	81.7	1.117	0.00061	1083.	−3.99	1450	1542
Cr	52.01	2200	89.4	0.987	−0.0018	1580.	−0.2	1500	1190
Si	28.06	2600	85.0*	0.585	0.00028	1420.	−1.94	1550	—
Au	197.2	2680	90.7	1.855	0.0016	1063.	−5.0	1600	1445
Ni	58.69	2900	98.1	1.066	0.00067	1454.	−3.12	1800	1717
Fe	55.85	3200	96.5	1.034	0.00155	1530.	−2.77	1850	1694
Pt	195.23	4300	125.	1.848	0.00231	1765.	−3.98	2400	2332
Mo	95.95	3700	156.	1.386	−0.00100	2620.	−0.87	2600	2755
C	12.01	(4000)	170.*	0.032	−0.0025	3600.	1.7	2900	—
Wo	183.92	5900	210.*	1.810	0.00076	3400.	−2.2	3800	3505
SiO_2(A)	60.06	2590	190.8	1.319	−0.01145	1710.	−6.0	2200	—
SiO_2(B)	60.06	—	95.4	1.319	−0.01145	—	—	1200	—
SiO_2(C)	60.06	—	127.2	1.319	−0.01145	—	—	1550	—

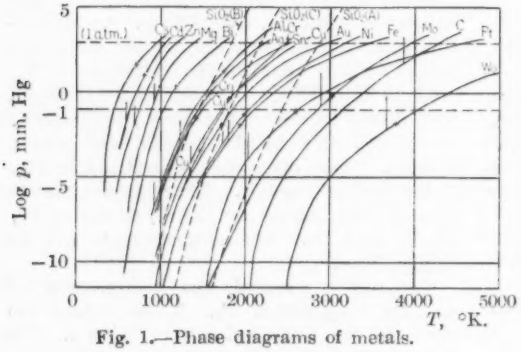

Fig. 1.—Phase diagrams of metals.

pressure curves in Fig. 1 (marked with +) show, however, that these temperatures correspond roughly to 10^{-1} mm. Hg of pressure, though the pressure is somewhat higher than 10^{-1} mm. Hg for volatile metals owing to the "over-heating". According to this fact, it is concluded that the vapor pressure near the specimen (10^{-1} mm. Hg) is usually not equal to the pressure in the vessel distant from the specimen (10^{-5} mm. Hg). This circumstance will be discussed later in detail. Temperature corresponding to the vapor pressure 10^{-1} mm. Hg is obtained from vapor pressure curve in Fig. 1, and cited on the ninth column as calculated values of vacuum evaporation temperature T_e. These agree well with values by Yarwood, excepting Al, Cr and Wo. It is commonly accepted that aluminum evaporates more easily than silver or chromium. This fact coincides with the calculated evaporation temperature, while Yarwood's values show that aluminum evaporates at higher temperature than silver or chromium. Some questions remained concerning this point. Data on silica, discussed in the preceding paper[2], are also cited in Table 1 and Fig. 1. From the Table and Fig., it is seen that quartz, SiO_2(A), evaporates at 2200°C. or with as great difficulty as platinum, while idealized silica gel, SiO_2(B), evaporates at 1200°C., or as easily as silver. The vacuum

evaporation temperature of actual silica gel, SiO_2(C), is estimated to be 1550°C., which is nearly equal to that of chromium or gold, and also coincides with experience.

Although the technique of vacuum evaporation is frequently used in electron microscopy, little has been discussed from the physicochemical point of view, so that even an approximate estimation will bring forth some contributions. To evaluate the rate of evaporation, the following assumptions are made. The molecules of an evaporating specimen fly away straightly in every direction with the mean square velocity:

$$\bar{v}=\sqrt{3RT/M}=15800\sqrt{T/M} \quad \text{(cm./sec.)}. \tag{7}$$

At a point, apart enough from the specimen, collisions between specimen molecules are, therefore, negligible, as long as collisions between specimen molecules and air molecules are negligeile. This latter is easily verified as follows. Let the number of collisions with air molecules done by one specimen molecule in unit time be Z, then,

$$Z=\pi\left(\frac{\sigma+\sigma_a}{2}\right)^2\cdot\sqrt{\bar{v}^2+\bar{v}_a^2}\cdot n_a, \tag{8}$$

where σ and σ_a are collision diameters of specimen and air molecule, respectively, and both are considered to be nearly equal to 3 Å. $\bar{v}$ and $\bar{v}_a$ are mean square velocities of specimen and air molecules, the values of which are obtained by the insertion of each value of temperatures and molecular weights into Eq. (7). n_a is the number of air molecules in unit volume and is expressed with the pressure p_a (mm. Hg) in the vessel by the equation:

$$n_a=p_a/k\,T_a. \tag{9}$$

The mean free path of specimen molecule in this air, λ, is given by

$$\lambda=\bar{v}/Z. \tag{10}$$

Since silica gel, as an example, evaporates at $T_s=1830$°K., and its molecular weight is $M_0=60$, the mean free path in air, where $T_a=293$°K. and $M_a=28.8$ are calculated by

$$\lambda=0.96\times10^{-2}/p_a \tag{11}$$

If $p_a=10^{-4}$ or 10^{-5} mm. Hg, then $\lambda=96$ or 960 cm., respectively. Under the usual experimental conditions, therefore, the probability of collision between specimen molecule and the air is safely omitted.

The number of specimen molecules in unit volume, n, placed at a distance r from the specimen is to be calculated as follows. Imagine a spherical shell of radius r, thickness dr, and volume $4\pi r^2dr$. Then the time required to pass through this shell by a molecule of velocity $\bar{v}$ is $(dr/\bar{v})$. The number of molecules evaporated in unit time is $-(N_A/M)\times(dw/dt)$, where w is the weight of specimen (g.), and N_A is Avogadro's number, so the number of specimen molecules in the shell is $-(N_A/M)(dw/dt)\times(dr/\bar{v})$. Therefore,

$$n=-(N_A/M)\times(dw/dt)/(4\pi r^2\bar{v}). \tag{12}$$

Let the temperature of a specimen be T_0 and the vapor pressure corresponding to it be p_0. The density of this vapor, n_0, is

$$n_0=p_0/k\,T_0. \tag{13}$$

The specimen is surrounded by the layer of such vapor, but the thickness of the atmosphere is assumed to be very slight. Then, in Eq. (12), $n=n_0$ if $r=r_0=$the radius of the specimen itself. The rate of evaporation becomes, therefore,

$$-dw/dt=4\pi r_0^2\bar{v}n_0(M/N_A). \tag{14}$$

From Eqs. (12) and (14),

$$n=n_0(r_0/r)^2. \tag{15}$$

That is to say, the vapor density n at a place distant as r from the specimen is greater when n_0 is greater, r is less, or r_0 is greater. n_0 becomes great when the temperature of specimen is high, since, in Eq. (13), p_0 increases exponentially when T_0 increases. If r_0 is great, the area of evaporation and the vapor density n are great.

When a shadow is cast using some metal as a specimen for electron microscopy, it is generally accepted that the shadow becomes diffuse if the pressure of air in the vessel is not low enough. Let us consider a unit area, of the distance l from the evaporating specimen, and of the angle of inclination θ to the direction of flying of a specimen molecule. Since the mean kinetic energy of a gas molecule is $(3/2)kT$, the sum of kinetic energy of a specimen molecule hitting this unit area per unit time, K_0, is

$$K_0=(3/2)kT_0n\bar{v}\sin\theta \tag{16}$$

where Eq. (15) is used for n, with $r=l$. While the sum of kinetic energy of air molecule hitting this area, K_a, is

$$K_a=(3/2)k\,T_a\,n_a(RT_a/2\pi M_a)^{1/2}. \tag{17}$$

It may be assumed that a shadow is clearly cast if $K_0 > K_a$, while the shadow becomes diffuse by the disturbance of air if $K_0 < K_a$. The value of l corresponding to $K_0 \simeq K_a$ is written as l_c:

$$l_c \simeq \left(6\pi \frac{T_0 M_a}{M_0 T_a}\right)^{1/4} (\sin\theta)^{1/2} r_0 (p_0/p_a)^{1/2}. \quad (18)$$

If the distance between the evaporating specimen and the area, where the shadow is to be cast, l is smaller than l_c, then a clear shadow will be obtained, and if l is greater than l_c, a diffuse shadow will be obtained. Let us assume, following ordinary experimental conditions, that $T_a = 293°\mathrm{K.}$, $M_a = 28.8$, $\sin\theta = 1/5$, $r_0 \simeq 10^{-1}$ cm., and $p_0 \simeq 10^{-1}$ mm. Hg. The calculated value of l_c is cited in Table 2 for some metals. It is seen that the value of l_c is about 1 cm. when the pressure of air in the vessel p_a equals 10^{-3} mm. Hg, and l_c is about 10 or 14 cm. for $p_a = 10^{-5}$ mm. Hg. In ordinary conditions, that is l is 6 cm. or so, a clear shadow will be obtained if the vacuum in the vessel is more than 10^{-4} mm. Hg, while the shadow will be disturbed if the vacuum is less than 10^{-4} mm. Hg. According to Eq. (18), it is understood that a clear shadow is easily obtained, if p_a is small by a sufficient preliminary evacuation, if p_0 is great by the high temperature of evaporating specimen, and if angle θ is not too small. These conclusions coincide with common experiences.

The rate of evaporation of a specimen has been given by Eq. (14). This is integrated with the equation:

$$(4/3)\pi r_0^3 \rho = w \quad (19)$$

and the time τ (sec.) required to evaporate w_0(g.) of the specimen completely is obtained as

$$\tau = \left(\frac{3\rho^2}{4\pi}\right)^{1/3} \left(\frac{RT_0}{M\bar{v}p_0}\right) w_0^{1/3} \quad (20)$$

where ρ is the density of the specimen. In the case of silica gel, it is assumed that $\rho = 2.2$, $M = 60$, $T_0 = 1830°\mathrm{K.}$, $\bar{v} = 8.73 \times 10^4$ cm./sec. and $p_0 = 10^{-1}$ mm. Hg, and

Table 2

Metals	M_0	T_0, °K.	l_c, cm. $p_a = 10^{-3}$ mm. Hg.	10^{-4} mm. Hg.	10^{-5} mm. Hg.
Al	27	1410	1.4	4.4	14
Ag	108	1440	1.0	3.2	10
Cr	52	1740	1.3	4.1	13
Au	197	1860	0.9	2.7	9
Ni	59	2040	1.3	4.4	13

for $w_0 = 5$ mg., $\tau = 39$ sec. (21)

is obtained. This agrees well with the experimental data cited in the preceding paper[2], that is 4~8 mg. of silica gel requires 20~40 sec. for evaporation.

Concerning the Eq. (20), two facts should be emphasized. The one is that the temperature of evaporation in a vacuum is defined as the temperature corresponding to the vapor pressure $p_0 = 10^{-1}$ mm. Hg. This is only a conventional definition and has no theoretical meaning. The time required to evaporate 5 mg. of silica gel is calculated for various temperatures and depicted on Fig. 2. As easily seen from this Figure, time τ increases enormously if the temperature is somewhat lowered from the evaporation temperature $T_e = 1830°\mathrm{K.}$ It is, therefore, concluded that the definition of T_e is significant practically. The second is that the rate of evaporation is mainly affected by the temperature of the evaporating specimen T_0, since the pressure p_0 is only dependent on T_0 for a given substance. The pressure of air in the vessel p_a, as far as $p_a < p_0$, is of least importance for evaporation velocity, although the distinctness of the shadow cast is largely affected by p_a.

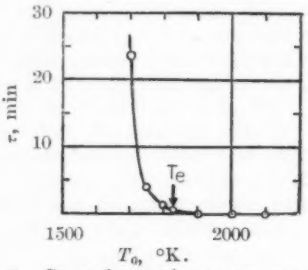

Fig. 2.—Dependence of τ on temperature.

The temperatures of tungsten filament and silica gel are directly measured by an optical pyrometer under the ordinary experimental condition of evaporation. The temperature obtained by the optical pyrometer is "brightness temperature" or "black body temperature". The emissivity of the substance should be known to recalculate the black body temperature to actual temperature[9]. As for tungsten, the data necessary to this correction are given for 0.665 μ of wave length of light[10]. As for silica gel, no data are given on its

(9) Edited by American Institute of Physics, "Temperature; Its Measurement and Control in Science and Industry," 1941, p. 1129.

(10) International Critical Tables, Volume V, pp. 243 and 245.

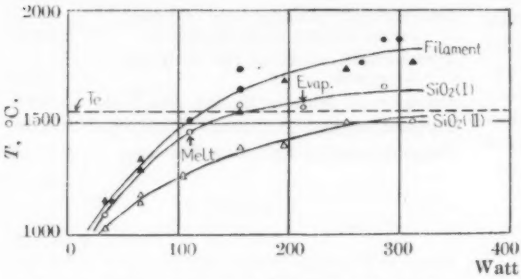

Fig. 3.—Temperature of filament and specimen.

emissivity. For a convention, the calibration curve for tungsten is also used for silica gel. The relation between electric power (watt) used and temperature observed are depicted in Fig. 3. The apparatus for evaporation and tungsten filament used are the same as reported in the preceding paper[2]. The relation between the temperature of tungsten filament and electric power used varies with the length of tungsten wire and the manner of its coiling. The data cited are examples. Five mg. of silica gel are used. When a piece of silica gel is placed in the bottom of a tungsten basket, it melts at about 1450°C. and evaporates at 1600°C., as shown in the Fig. 3 as SiO_2(I). This agrees with the estimated evaporation temperature cited in Table 1. While the piece is placed on the upper part of the basket, it cannot be made to evaporate by less than 300 watts heating as shown as SiO_2(II). This fact should be remembered when an evaporation experiment is done.

Whether the substance evaporates after fusion or sublimates without fusion may have some significance in the rate of evaporation, since the melted substance adheres to the filament, and high temperature will readily be obtained. For example, the evaporation of silver is far easier than that of chromium. The main reason for this will be that the evaporation temperature shown in Table 1 of silver is even 300°C. lower than that of chromium. However, there may also be another reason that silver evaporates after fusion while chromium sublimates without fusion.

Summary

Phase diagrams are drawn for many metals under some approximations, and "vacuum evaporation temperature" is estimated as the temperature corresponding to 10^{-1} mm. Hg of vapor pressure. This temperature agrees well with that given by Yarwood. The rate of evaporation is calculated, and the result agrees well with experience, at least, for silica gel. As for shadow casting, it is concluded that high temperature of specimen and low pressure of air in the vessel are the necessary conditions to obtain clear shadow. The temperature of evaporating silica gel is measured with optical pyrometer, and a satisfactory result is obtained.

Chemical Institute, Faculty of Science, the University of Tokyo, Tokyo

Gehalt an Molybdän in Japanischen Vulkanischen Gesteinen

Von Tomitaro ISHIMORI

(Eingegangen am 12, Juni 1951)

Über den Gehalt an Molybdän in europäischen Eruptivgesteinen wurden schon einige Untersuchungen ausgeführt[1],[2]. Einige Bestimmungen des Molybdäns wurden auch ausgeführt über verschiedene Tiefseetone[3] und Kohlenaschen[1]. Vor kurzem versuchte I. Iwasaki[5] die Bestimmungen des Gehaltes an Molybdän in mehreren japanischen Gesteinen. Aber, aus dieselben Untersuchungen erkannte er dass man die grössere Menge der Gesteinsprobe braucht um die genaueren Zahlen zu gewinnen, denn das Gehalt an Molybdän sind

(1) I. und W. Noddack, *Z. Physik. Chem.*, **A 154**, 207 (1931).
(2) G. von Hevesy und R. Hobbie, *Z. anorg. allgem. Chem.*, **121**, 142 (1933).
(3) S. Oana, *J. Chem. Soc. Japan*, **59**, 1234 (1938); K. Kuroda, *ibid.*, **63**, 496 (1942).
(4) I. Iwasaki, unveröffentlicht.
(5) I, Iwasaki, "Chemistry of Volcanoes" 1948, S. 182.

sehr niedrig in japanischen vulkanischen Gesteinen (0.0001～0.0002 % MoO_3). In vorliegender Mitteilung berichte ich über die experimentellen Resultate meiner Bestimmung über den Gehalt an Molybdän in japanischen vulkanischen Gesteinen mit grösserer Menge der Probe (5～10 g.).

Methode der Bestimmungen

Sandellsche kolorimetrische Methode[6] für die Bestimmung von Molybdän in Silikatgesteinen wurde mit einigen Modifizierungen angewendet.

Etwa 5-10g. feingepulverte Probe wurde in einem Platintiegel mit fünfmalem Natriumkarbonat genug geschmolzen. Die Schmelze wurde mit Wasser digeriert unter Zusatz von einigen Tropfen des Äthylalkohols. Der Niederschlag wurde dann abfiltriert und mit Wasser verdünnt zum definierten Volum um je 100 cc. Lösung 1 g. Probe zu enthalten.

Je 100 cc. Lösung wurde in Scheidetrichter mit 16 cc. konzentrierter Salzsäure, 6 cc. 5-prozentigem Kaliumrhodanat und 6 cc. 10-prozentigem Zinn-(II)-chlorid behandelt, dann mit 20 cc. Äther (behandelt mit Kaliumrhodanat und Zinn-(II)-chlorid) geschüttelt. Das Molybdän geht in die Schicht von Ätherlösung über. Die Ätherlösung wurde abgetrennt und verdünnt zum 20 cc. Volum unter Zusatz von neuem Ätherreagens.

Die zweite 100 cc. Lösung der Probe wurde nach gleicher Behandlung wieder mit oben-erwähnter 20 cc. Ätherlösung geschüttelt. Nach einer Reihe von dieselben Behandlungen wurde alles Molybdän in Form von $K_2[MoO(CNS)_5]$[7] in einem kleinem Volum von Ätherlösung gesammelt. Die rote Färbung der Ätherlösung wurde mit der Färbung der Lösung des bekannten Gehaltes an Molybdän kolorimetrisch vergleicht.

Resultat

Die Bestimmung über drei Durchschnittmischungen und drei Gesteinsproben wurden ausgeführt. Die Resultate sind in Tabelle 1 zusammengefasst.

Tabelle 1

Probe	% MoO_3
Durchschnittmischung von 10 japan. Basalten	0.00014
Durchschnittmischung von 15 japan. intermediären Ergussgesteinen	0.00017
Durchschnittmischung von 10 japan. Lipariten	0.00045
Olivinbasalt (Shimo-Oimura, Shizuoka)	0.00008
Hypersthendazit (Yugawara, Kanagawa)	0.00027
Nephelinbasalt (Nagahama, Shimane)	0.00026

Tabelle 2

	g. Mo/g.
Sauer Schluchsee Granit (Schwarzwald)	1.2×10^{-5}
Mischung von 282 Eruptivgesteinen	1.5×10^{-5}
Gemisch aus 67 Gabbros und Noriten sehr verschiedener Herkunft	0.3×10^{-5}

Aus Tabelle 1, wissen wir dass die vorliegenden Resultate mit den Iwasakischen Resultaten[5] genau übereinstimmen.

V. M. Goldschmidt[8] gab 15 g. Mo/ton für Eruptivgesteinen an und I. und W. Noddack[1], in 1931, 0.00 n % Mo für europäische Basalte. In der Vergleichung mit diesen Resultaten, sind die Werte an Molybdän in japanischen vulkanischen Gesteinen sehr niedrig. Es sei noch erwähnenswert dass die Bestimmungen von Olivinbasalt und Durchschnittmischung von japanischen Basalten nur niedrige Werte des Gehaltes ermittelten, während sich die von Nephelinbasalt einen bemerkbaren grossen Gehalt ergaben. Hier muss man berücksichtigen, dass das Nephelinbasalt die grossen Verschiedenheiten, vergleicht mit den normalen japanischen vulkanischen Gesteinen, auch in anderen mehreren chemischen Bestandteilen zeigt.

Die Resultate der Untersuchung von G. von Hevesy und seiner Mitarbeiter[2] zeigten die Anreicherung des Molybdäns in saueren Eruptivgesteinen (Tabelle 2). Die Neigung stimmt mit der Resultaten meiner Untersuchung überein.

Herrn Prof. I. Iwasaki bin ich für die Anregung zu dieser Arbeit und für seine zahlreichen Ratschläge zu grossem Dank verpflichtet.

Chemisches Institute, Naturwissenschaftliche Fakultät, Kyushu Universität, Fukuoka, Japan

(6) E. B. Sandell, *Ind. Eng. Chem., Anal. Ed.* **8**, 336 (1936).

(7) Y. Uzumasa und K. Doi, Dies Bulletin, **14**, 337 (1939).

(8) V. M. Goldschmidt, "Geochemische Verteilungsgesetze der Elemente," IX (1938).

6

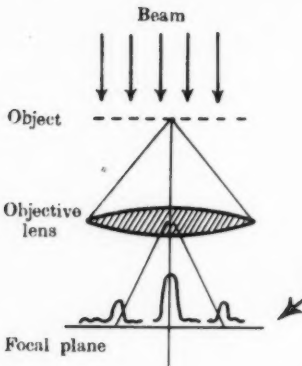

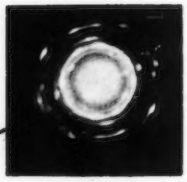

Fig. 1.

Fig. 2.

Fig. 1.—Diffraction pattern obtained by the electron beam running perpendicular to the replica film of Fig. 2.

Fig. 2.—Micrograph of the oxide replica formed on iron single crystal.

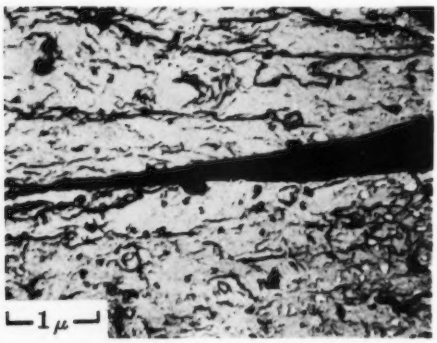

Fig. 4.—Micrograph of the sulphide replica formed on silver plate.

[*To face page 253.*